CHALMERS
UNIVERSITY OF TECHNOLOGY

SCIENTIFIC REPORT

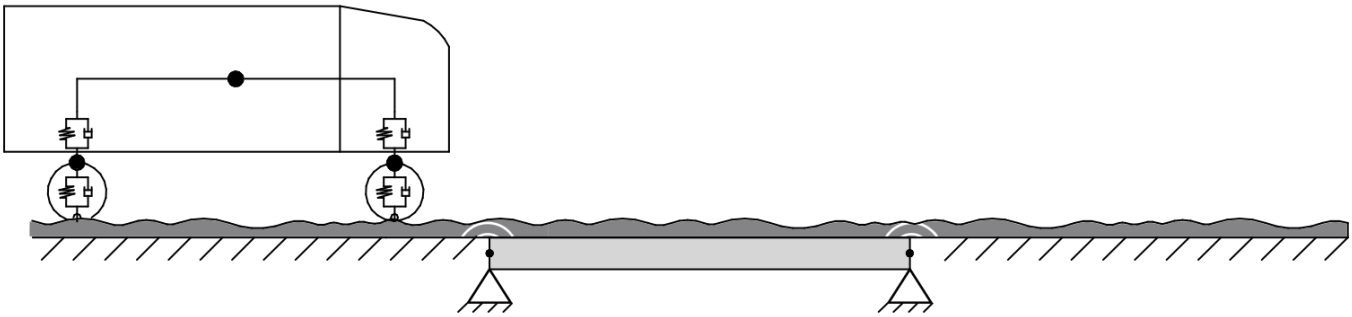

Pre-study of Dynamic Amplification Factor for Existing Road Bridges

CHRISTOFFER SVEDHOLM
VIKTOR ERIKSSON
MARIO PLOS
MATS KARLSSON

DEPARTMENT OF ARCHITECTURE AND CIVIL ENGINEERING
Division of Structural Engineering
Concrete Structures

CHALMERS UNIVERSITY OF TECHNOLOGY
Report ACE 2022:1
Gothenburg, Sweden 2022
www.chalmers.se

REPORT ACE 2022-1

Pre-study of Dynamic Amplification Factor for Existing Road Bridges

CHRISTOFFER SVEDHOLM
VIKTOR ERIKSSON
MARIO PLOS
MATS KARLSSON

CHALMERS
UNIVERSITY OF TECHNOLOGY

Department of Architecture and Civil Engineering
Division of Structural Engineering
Concrete Structures
Chalmers University of Technology
Gothenburg, Sweden 2022

Pre-study of Dynamic Amplification Factor for Existing Road Bridges
CHRISTOFFER SVEDHOLM
VIKTOR ERIKSSON
MARIO PLOS
MATS KARLSSON

Report ACE 2022-1
Institutionen för arkitektur och samhällsbyggnadsteknik
Chalmers tekniska högskola, 2022

Department of Architecture and Civil Engineering
Division of Structural Engineering
Concrete Structures
Chalmers University of Technology
SE-412 96 Göteborg
Sweden
Telephone +46 31 772 1000

Department of Architecture and Civil Engineering
Gothenburg, Sweden 2022

Pre-study of Dynamic Amplification Factor for Existing Road Bridges
CHRISTOFFER SVEDHOLM
VIKTOR ERIKSSON
MARIO PLOS
MATS KARLSSON
Department of Architecture and Civil Engineering
Chalmers University of Technology

Abstract

The Swedish Road network has, since 2018, been divided into four bearing capacity classes (BKs)—BK1–BK4. The heaviest allowed gross vehicle weight increased when BK4 was introduced, from 64 tonnes (BK1) to 74 tonnes (BK4). The Swedish Transport Administration aims, by 2025, to classify 60 % of the strategic road network for the heavy transport industry as BK4, increasing to 70–80 % by 2029. However, to reach these goals, it is estimated that over 700 bridges will need to be strengthened or replaced.

This study, using a site-specific investigation to calculate the assessment dynamic ratio (ADR), showed that some of these bridges could be upgraded to BK4. A review of the literature indicated that light vehicles tend to have high dynamic amplification factors (DAFs), but light vehicles do not have critical load effects and are therefore not relevant from a design perspective. Instead, heavy vehicles are critical for the design. Both experimental and analytical investigations have shown that heavy gross vehicle weights result in low DAF values.

This report proposes effective ways to collect site-specific dynamic traffic load information and a methodology to produce site-specific dynamic allowances using both experimental measurements and numeric models. It also explains how this methodology can be adopted by transportation agencies to study bridges along transport corridors.

Findings from the pre-study have resulted in the following research proposals: site-specific field measurements to quantify DAFs, guidelines for numerical modelling of vehicle–bridge interactions (VBIs), DAF for each limit state, three–dimensional analysis of VBIs, the introduction of gross vehicle weight into DAF equations, and pilot tests of proposed frameworks for transport corridors. The authors believe that several topics can be covered within the framework of a PhD project.

Keywords: Dynamic Amplification Factor, Assessment Dynamic Ratio, Load-Carrying Capacity Assessment, Transport Corridor, Site-Specific Dynamic Allowance, Gross Vehicle Weight, Heavy Transport.

Preface

This pre-study was financed by the Swedish Transport Administration (Trafikverket) and ELU Konsult. The report was compiled by Viktor Eriksson and Christoffer Svedholm from April 2020 to December 2021. Mario Plos (Chalmers) and Mats Karlsson (Trafikverket/Chalmers) provided useful comments during monthly progress meetings and reviewed the manuscript and commented and proofread the final version. Last but not least, we gratefully acknowledge the valuable contribution from the reference group: Ebbe Rosell (Trafikverket), Costin Pacoste (ELU Konsult/KTH), Lennart Cider (Volvo), Torsten Wiborg (Sveaskog), Andreas Andersson (Trafikverket/KTH) and Daniel Cantero (NTNU).

Contents

List of Figures

List of Tables

1
INTRODUCTION

1.1 Background

Since 2018, the Swedish road network has been divided into four BKs (BK1–BK4). The heaviest allowed gross vehicle weight increased when BK4 was introduced, from 64 tonnes (BK1) to 74 tonnes (BK4). A detailed investigation performed by Natanaelsson and Ngo (2015) concluded that the introduction of BK4 will provide environmental benefits and strengthen the Swedish industry. Kalman and Ullberg (2020) supported this claim, explaining that a fully loaded 74-tonne-truck has 13 % more payload than a 64-tonne-truck and that the fuel consumption per tonne of transported goods would decrease by 6 %. Today, 95 % of the public Swedish road network is classified as BK1 (Trafikverket, 2019), but only 20 % is classified as BK4 (Natanaelsson and Eriksson, 2020). The heavy transport industries (e.g. timber and steel) are eager for the Swedish Transport Administration to upgrade more bridges to BK4 due to the previously mentioned benefits. Considering the gross vehicle weight trend over time (Figure 1.1), it is likely that the Swedish Transport Administration will indeed increase the allowed gross vehicle weight. This possibility is strengthened by the news that Volvo Lastvagnar has produced 90-tonne trucks for the steel industry (Volvo Lastvagnar, 2018). The ambition of the Swedish Transport Administration is to upgrade the whole BK1 road network to BK4 in the future. The goal for the year 2025 is to classify 60 % of the strategic road network for the heavy transport industry as BK4, increasing to 70–80 % by the year 2029; however, to reach these goals, Natanaelsson and Eriksson (2020) estimated that over 700 bridges will need to be strengthened or replaced.

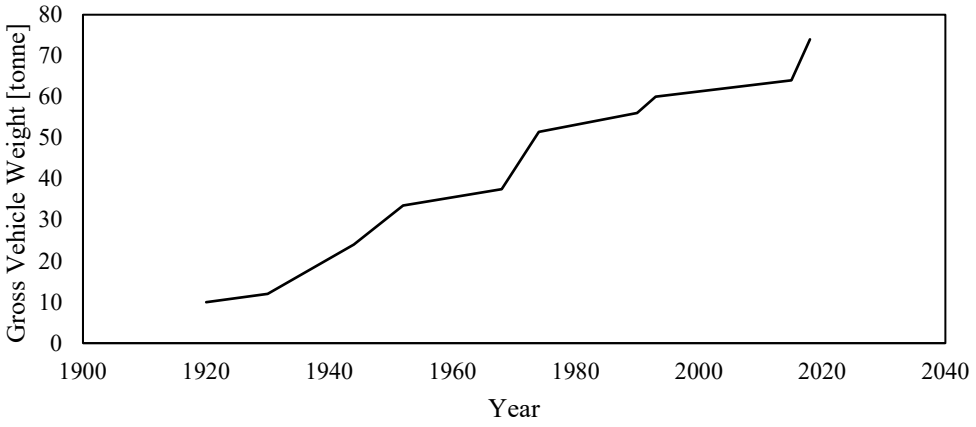

Figure 1.1: Gross vehicle weight trends over time.

When performing a load-carrying capacity assessment to upgrade a BK1 bridge to BK4, the dynamic contribution of the vehicles must be taken into account. The contribution is calculated using an empirical equation to provide a percentage value for the vehicle's axle load, which is added to the total axle load. The equation has been used at least since the late 1990s (Vägverket, 1998), and the same percentage value is used for all gross vehicle weights, meaning that, for light vehicles, this will not result in a high contribution to the vehicle's total load in tonnes, but for heavier vehicles, the contribution will be relatively heavy and will be a crucial factor for upgrading bridges to a higher BK.

1.2 Aim and scope

It is well known that a modern vehicle suspension system reduces vibration levels and improves drivers' comfort. Dialogue with the truck manufacturing industry has led to the belief that a modern suspension system may also reduce bridge vibration.

The aim of this pre-study was to investigate whether field measurements and numerical models could be used to predict the dynamic response of road bridges more accurately. The specific objectives were:

1. Summarise existing methods for load-carrying capacity assessment.
2. Identify the most important factors that affect the dynamic response.
3. Present state-of-the-art methods to determine site-specific dynamic allowances.
4. Present a framework for implementing this procedure in practice.

Based on the above-mentioned aims and scope, this paper formulates several research proposals.

1.3 Outline of the report

This report consists of eight chapters. Chapter 1 introduces the topic and explains the aims and scope of the study. Chapter 2 presents the Swedish regulations for structural designers and the traffic industry. Chapter 3 provides a brief introduction to the DAF, gives an historical review of the topic, and presents empirical equations recommended by various design codes. Chapter 4 explains VBIs and discusses in detail how road irregularities, gross vehicle weights, and vehicle models affect the results. This section explains the case simulations performed by the authors with the help of the MATLAB toolbox according to Cantero et al. (2016). Chapter 5 subsequently describes a methodology for calculating site-specific dynamic allowances. This methodology was first proposed for the EU SAMARIS and ARCHES projects. Chapter 6 introduces a workflow for load-carrying capacity assessments that incorporates site-specific dynamic allowances. Finally, Chapters 7 and 8, respectively, present the conclusions and research proposals.

The work performed by Bergenudd (2020), as a basis for this pre-study, is mentioned throughout the report but mostly in Chapters 3 and 4. Bergenudd calculated DAFs for road bridges based on numerical simulations performed using the MATLAB toolbox developed by Cantero et al. (2016).

2
CODE OF PRACTICE

New road bridges in Sweden are designed for traffic loads specified in EN 1991-2 (2002) and the National Annex TSFS 2018:57 (Transportstyrelsen, 2018a). These loads are intended to meet traffic loads from the traffic industry defined in Legal loading (Transportstyrelsen, 2018b). To examine the maximum vehicle weight of the different vehicles defined in Transportstyrelsen (2018a), a load-carrying capacity assessment with different traffic load scenarios is conducted according to TDOK 2013:0267 (Trafikverket, 2020). A bridge is then categorised into one of four BKs specified by the Swedish Transport Administration.

2.1 Load-Carrying Capacity Assessment Procedure of Bridges

There are two different traffic load models presented in Trafikverket (2020), namely special vehicles and heavy transports, which are used when a load-carrying capacity assessment of a bridge is performed in accordance with Trafikverket (2020). Special vehicles are 15 predefined vehicles with different configurations of single axles, tandem systems and triple axles. Heavy transports is used when specifically configurated and heavy vehicles pass a bridge. Two methods can be used to execute a load-carrying capacity assessment (Trafikverket, 2020). The first method is a comparison between the load effects from traffic load models used when designing the bridge and one of the two traffic load models mentioned above. The second method is a capacity analysis of the bridge when special vehicles or heavy transports cross the bridge. The aim is to classify a bridge for different types of traffic load scenarios (e.g. vehicles in traffic lanes or by themselves in the middle of the bridge) with the maximum load from a single axle (A) and tandem systems/triple axles (B). The procedure is described in Figure 2.1.

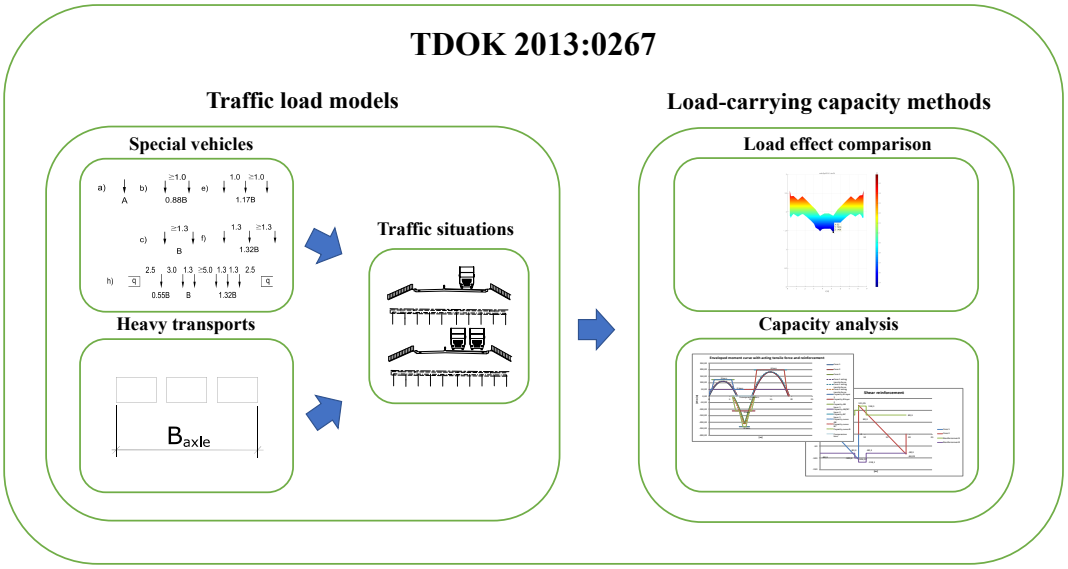

Figure 2.1: Procedure of the load-carrying capacity assessment in accordance with Trafikverket (2020).

The most commonly used traffic load model is special vehicles, which consist of 15 vehicles called a) to o). The first six vehicles comprise a single axle (a), a tandem system(b–d) or a triple axle (e–f), with various amplitudes and distances between the axles, see Figure 2.2. The other vehicles, or road trains, are a combination of axle systems, see Appendix A.

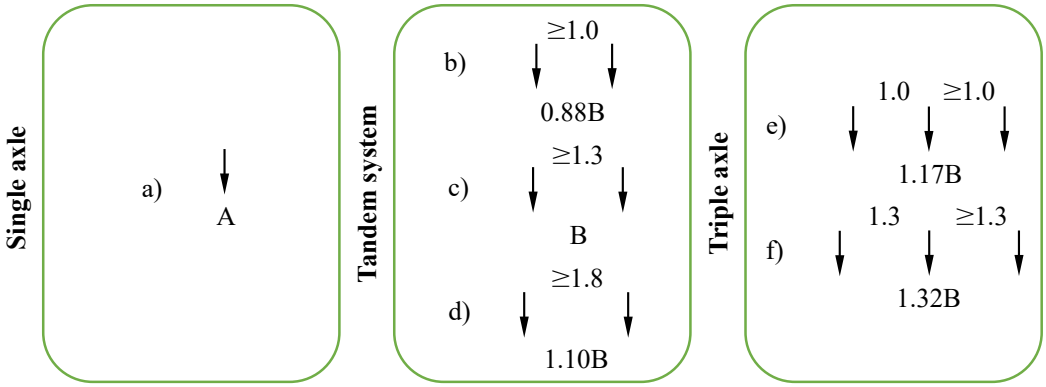

Figure 2.2: Special vehicles a)–f). Load and distance [m] between axles for a single axle, tandem systems and triple axles according to Trafikverket (2020).

Dynamic amplification, expressed by the impact factor (IF), is added to the point loads and is calculated by:

$$\mathrm{IF}_{\mathrm{TDOK}} = \frac{180 + 8(v - 10)}{20 + L} \leq 35[\%] \tag{2.1}$$

where L [m] is the span length, and v is the vehicle speed set to 80 km/h. The carriageway on a bridge is divided into a maximum of four traffic lanes 3 m wide each. A maximum of two lanes can be used by the special vehicles. Vehicle loads in

the first lane are multiplied by a factor of 1.0 and vehicle loads in the second lane by 0.8. The remaining lanes are loaded with a uniformly distributed load (q), which is set to either 0 kN/m or 5 kN/m. The transverse distance between wheels varies between 1.7 m and 2.3 m. Three different traffic situations are investigated. Special vehicles shall cross the bridge in the traffic lanes, in the middle of the carriageway by themselves and in the middle of the carriageway with traffic on the opposite carriageway, see Figure 2.3.

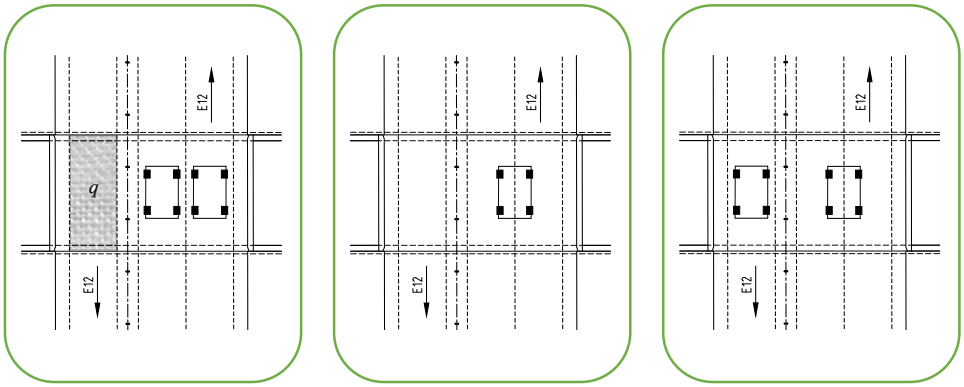

Figure 2.3: Special vehicles in the traffic lanes (left picture), in the middle of the carriageway by themselves on the bridge (middle picture) and in the middle of the carriageway with traffic on the opposite carriageway (right picture).

During special occasions when heavy and non-ordinary vehicles (i.e. axle systems and configurations not covered by the special vehicles) pass a bridge, a load-carrying capacity assessment for heavy transports is required. The bridge is then checked for a specifically defined vehicle, with known dimensions, number of axles and axle loads. Before the vehicle is allowed to cross the bridge, an application needs to be sent together with the specifications of the vehicles' configuration. The distribution of traffic lanes is the same as that for special vehicles, but the width of the traffic lane can vary depending on the width of the vehicle. The minimum width is set to 3 m. Two different traffic situations are considered: the defined vehicle passes the bridge 1) in the traffic lanes at the same time as special vehicles and 2) by itself.

When special vehicles passes the bridge along with the defined heavy vehicle, a factor of 0.8 is used for the special vehicles. The remaining lanes are loaded with the uniformly distributed load q. The IF for heavy transports is calculated using Eq. 2.1, and the vehicle speed is set to the actual velocity. If the vehicle speed is less than 10 km/h, the IF is set to 0. The IF for the special vehicles is calculated by Eq. 2.1 with the vehicle speed set to 80 km/h and the maximum IF is limited to 35 %.

The load-carrying capacity assessment of a bridge, using the traffic load models described above, can be performed either with a load effect comparison or a capacity analysis. In a load effect comparison, the designed load effect in the ultimate limit state, with traffic loads according to EN 1991-2 (2002) and Transportstyrelsen (2018a) is compared with the load effect from the traffic models and scenarios de-

scribed above. The A and B values are then scaled up or down in proportion to the load effect. This method is used for newer bridges designed with traffic regulations not older than from 2009. The Swedish Transport Administration's automated bridge check program Brokontroll can be used for heavy transports. The user specifies the configuration of the specifically defined vehicle, and the program checks the vehicle against the existing A and B values determined for the actual bridge.

For older bridges, capacity analysis are used instead. Normally, the load effect in every cross-section of a bridge is compared to corresponding cross-sectional capacity, for ultimate and serviceability limit states, to evaluate the maximum A and B values for the traffic loads and scenarios according to Trafikverket (2020). In some cases, more advanced analysis methods have been used to assess the load-carrying capacity. The assessment can then be enhanced successively using improved knowledge of the bridge, better analysis methods and more advanced safety verification, see e.g. the European project Sustainable Bridges (Bien et al., 2007) and Plos et al. (2021). Improved knowledge can be obtained through more detailed inspections, testing and monitoring. Better analysis methods include improved structural analysis and resistance models on higher levels of approximations. Examples of non-linear analysis for enhanced structural assessment is found in e.g. Plos (2002) and in Plos et al. (2021). Here, it was demonstrated that 15 % to 35 % higher capacity can be shown through non-linear finite element analysis of reinforced concrete slabs. The safety index method have been used by e.g. Carlsson and Karoumi (2008), who performed a load-carrying capacity assessment of Ölandsbron. By monitoring the actual traffic flow and using the safety index method instead of performing a traditional load-carrying capacity assessment, it was possible to increase the B value by 27 %. Emanuelsson and Persson (2011) conducted a load-carrying capacity assessment of an existing concrete slab frame bridge. The bridge was built during the expansion of road E6 in 1959. Using the safety index method with the traffic load model called special vehicles defined in Trafikverket (2020), they showed increases of 6.6 % and 8.0 % for the A and B values, respectively.

The Swedish public road network is categorised into four BKs (Transportstyrelsen, 2018b). BK1 and BK4 are for higher vehicle weights, and the regulations are in accordance with EU standards. Each bridge is classified by the Swedish Transport Administration, depending on the results of a load-carrying capacity assessment. The A and B values for each BK are presented in Table 2.1. For BK4, the B values depend on the span length of the bridge, while it is independent of the span lengths for the other BKs.

Table 2.1: A/B values in tonnes according to the different BKs used by the Swedish Transport Administration to classify a bridge. The BK4 values are set by Trafikverket (2018a).

Span length [m]	**BK1**	**BK2**	**BK3**	**BK4**
≥ 11.5	12/19*	10/16	8/12	12/21
$6.0 \leq$				12/19*

*With the use of air suspension, otherwise 12/18.

2.2 Traffic Industry Regulations

Vehicles that run on the Swedish public road network are categorised according to the vehicles' weight, width and distance between axles (Transportstyrelsen, 2018b). Figure 2.4 shows the loads from a single axle, tandem systems and triple axles described for the different BKs. BK1 and BK4 have the highest permitted loads, followed by BK2 and BK3. It can also be noted that BK1 and BK4 have the same permitted loads.

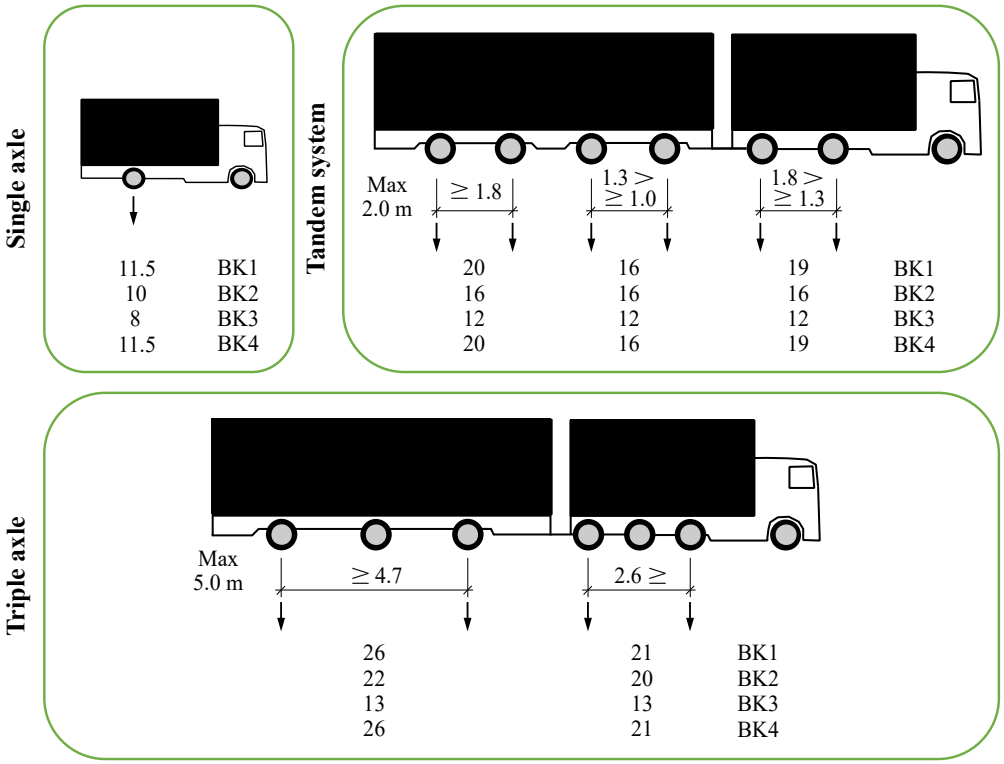

Figure 2.4: Distance [m] and maximum load [tonne] from single axle, tandem systems and triple axles (less than 2.6 m and more than 4.7 m), according to Transportstyrelsen (2018b).

As shown in the figure, there are no differences between BK1 and BK4. The difference between BK1 and BK4 is better visualised in Figure 2.5. BK1 and BK4 have the same maximum permitted gross weight up to a distance of 6.2 m in terms of distance between the first and last axle. For distances greater than 6.2 m, BK4 has a higher permitted gross weight than BK1. This means that a bridge no longer than 6.2 m classified as BK1 can also be classified as BK4. If a trailer or a dolly is coupled to a semi-trailer, BK1 and BK4 will have the same gross weight up to a distance of 7.8 m.

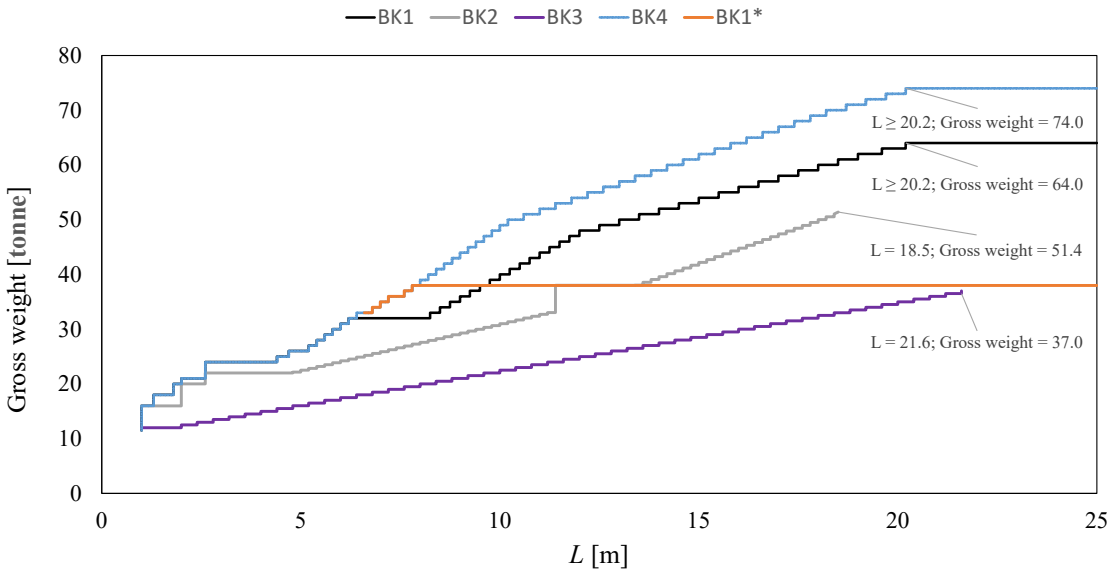

Figure 2.5: Maximum permitted gross weight for a vehicle or road train and the distance between the first and last axle of the vehicle or road train, according to Transportstyrelsen (2018b).
*In the event that a trailer or dolly is coupled to a semi-trailer, with a minimum distance between the first and last axles of 6.6 m.

2.3 Designed Traffic Load Models and Traffic Industry Regulations

As mentioned previously, the traffic loads used when designing new bridges are regulated to meet traffic loads from the traffic industry. Chapters 2.1 and 2.2 show a strong correlation between the load-carrying capacity assessment standard (Trafikverket, 2020) and industry regulations (Transportstyrelsen, 2018b) regarding the configuration of axle systems for the vehicles. Figure 2.6 presents the correlation between the first six special vehicles used for load-carrying capacity assessment and how the industry regulates the distances between the axles for the different axle systems. Each special vehicle can be matched with the regulations for the BK vehicles. The values in brackets are those used when a new bridge is designed, and they are higher than those for vehicles passing the bridges. To all point loads, an IF is set to at least 20 % (Transportstyrelsen, 2018a).

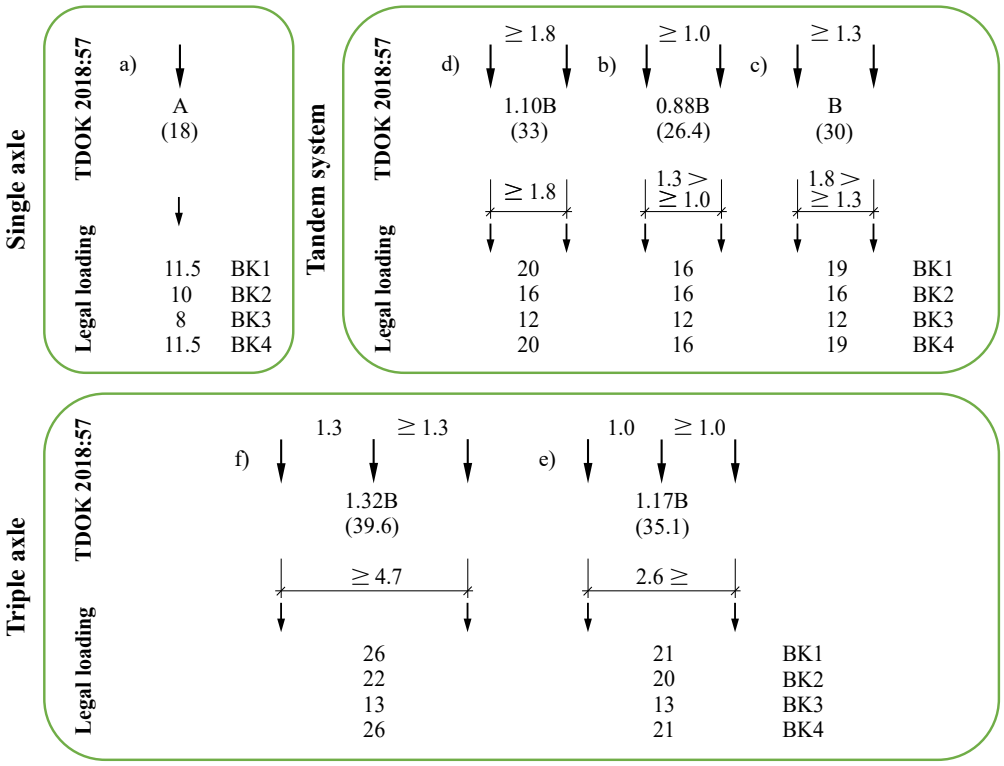

Figure 2.6: Distance [m] and maximum load [tonne] from a single axle, tandem systems and triple axles (less than 2.6 m and more than 4.7 m) according to Transportstyrelsen (2018b) compared with those from special vehicle a)–f) according to Trafikverket (2020), with loads from Transportstyrelsen (2018a) in ().

If the A and B values are expressed with values in tonnes in terms of the BK vehicle's loads, then vehicle a), which is expressed with the single A value, and vehicle c), which is expressed with the single B value, can be used and expressed as shown in Table 2.2. Table 2.2 also shows the values from Table 2.1 in terms of the BK for bridges. The A and B values comparing the BKs for vehicles and bridges are similar,

with BK4 being higher depending on the span length of the bridge. Comparing the A and B values for BK1/BK4 with TSFS 2018:57 shows that a new bridge is designed with around 50 % higher point loads regarding the loads from the six first special vehicles.

Table 2.2: A and B values in tonnes in terms of the different BKs for bridges and vehicles and when a new bridge is designed according to TSFS 2018:57 (Transportstyrelsen, 2018a).

	BK1	**BK2**	**BK3**	**BK4**	**TSFS 2018:57**
Vehicle BK	11.5/19	10/16	8/12	11.5/19	18/30
Bridge BK	12/19	10/16	8/12	12/21*	18/30

*Span length $\leq$ 6.0 m 12/19.

Both the traffic industry and the load-carrying capacity assessment standard regulate longer vehicles with combinations of the axle systems compared above. Figure 2.7 presents the three special vehicles g), h) and i) denoted as short truck, truck and long truck, respectively, with the total gross weight expressed as the B value. Their length in terms of the distance between the first and last axle is presented, which is how the traffic industry presents regulations on gross weight (see Figure 2.5). If each vehicle's total B value is multiplied by the corresponding B value of each BK in Table 2.2 for bridges, the total gross weight will be expressed in tonnes, as presented in Table 2.3. The lowest value for BK4 (B = 19) is used for the short truck to consider the span length. Truck and long truck are longer than 11.5 m, therefore, B = 21 is used. Table 2.3 also presents the allowed weight in terms of the distance, the maximum weight of all vehicles presented in Figure 2.5 and the weight of the vehicles when a new bridge is designed.

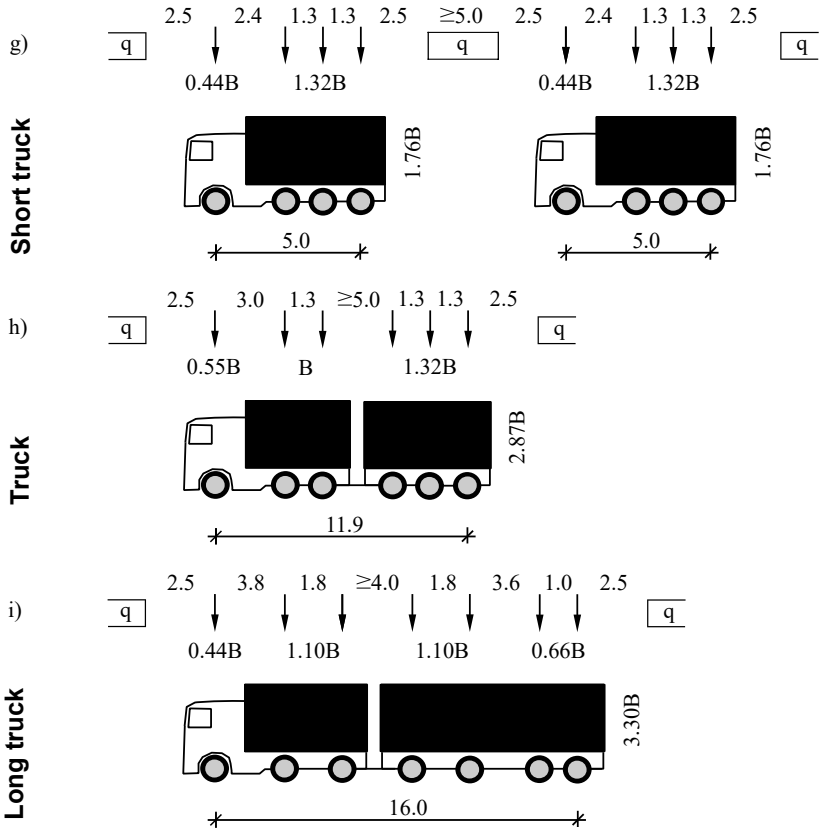

Figure 2.7: Special vehicles g) (short truck), h) (truck) and i) (long truck) according to Trafikverket (2020) with the total B value and length between first and last axle.

As shown in Table 2.3, no difference is found between BK1 and BK4 for the short truck. This means that in a load-carrying capacity assessment, BK1 and BK4 bridges shorter than 6.0 m are not considered different from each other. The BK values are always higher than the allowed weights. The values of a short truck are always at least 25 % higher; those of a truck are at least 15 % higher for BK1, BK2 and BK3 and 11 % higher for BK4; and those of a long truck are at least 10 % higher for BK1, BK2 and BK3 and 8 % higher for BK4.

Table 2.3: Maximum weight for a vehicle depending on the BK according to Transportstyrelsen (2018b) and when a new bridge is designed according to Transportstyrelsen (2018a). The total gross weight of short truck, truck and long truck compared with the allowed weight depending on the distance between the first and last axle according to Transportstyrelsen (2018b).

	BK1	**BK2**	**BK3**	**BK4**	**TSFS 2018:57**
Max. weight	64	51.4	37	74	106
Short truck	33.4	28.1	21.2	33.4	52.8
All. weight	26	22.5	16	26	-
Truck	54.5	45.9	34.4	60.2	86.1
All. weight	47	38	24.5	54	-
Long truck	62.7	52.8	39.6	69.3	99
All. weight	56	44.8	30	64	-

The values presented in Table 2.3 show potential to have heavier vehicles on classified bridges. Figure 2.8 shows the short truck, truck and long truck in terms of the allowed gross weight for every BK. For BK1/BK4, the area with the short truck (orange 'potential area') shows that a higher weight (around 28 % higher at a distance of 5 m) may be possible for vehicles up to a length of 6.8 m with respect to the allowed weight. The truck and long truck show a green potential area for BK1. A BK1 truck can be promoted to BK4, and a 6.7 tonne higher weight can be allowed for a BK1 long truck. The yellow area indicates that the BK4 weight can be increased for truck and long truck (6.2 tonnes higher for truck and 5.3 tonnes for long truck). Only having short truck and truck (special vehicles g) and h), respectively) for a load-carrying capacity assessment shows a large gap between 5 m and 11.9 m, which is not covered by any special vehicle. Introducing a new special vehicle with a length between 5 and 11.9 m may result in a more precise load-carrying capacity assessment for bridges within that length. For BK2 and BK3, all trucks have a higher weight than the allowed weight. A BK2 truck has a 20 % higher weight than the allowed weight, and a BK3 truck has a 40 % higher weight.

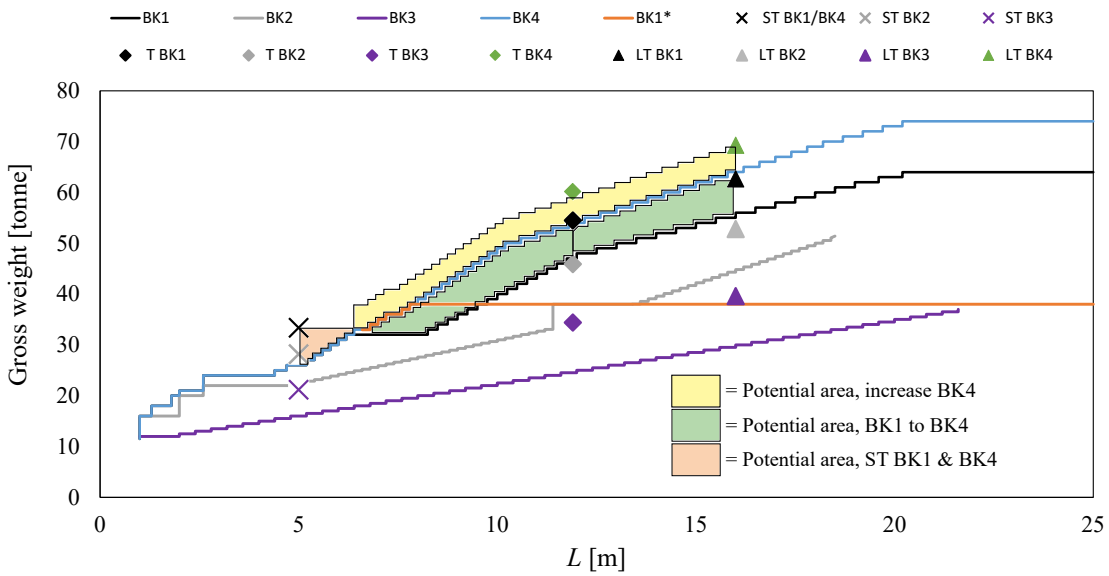

Figure 2.8: Allowed gross weight for BK1–BK4 with respect to the distance between the first and last axle according to Transportstyrelsen (2018b) and gross weight for short truck (ST), truck (T) and long truck (LT) with different BKs.
*In the event that a trailer or a dolly is coupled to a semi-trailer, with a minimum distance between the first and last axles of 6.6 m.

3

DYNAMIC AMPLIFICATION FACTOR

3.1 Introduction

When a vehicle crosses a bridge, the total deflection (y_{Total}) consists of a static (y_{Stastic}) and a dynamic (y_{Dynamic}) component:

$$y_{\text{Total}} = y_{\text{Static}} + y_{\text{Dynamic}} \tag{3.1}$$

The literature has posited several formulations for the dynamic component, one of which is to define y_{Dynamic} as a ratio of the static component ($y_{\text{Dynamic}} = \text{IF} \cdot y_{\text{Static}}$). Inserting this definition into Eq. 3.1 gives:

$$\text{IF} = \frac{y_{\text{Total}} - y_{\text{Static}}}{y_{\text{Static}}} \tag{3.2}$$

In Eq. 3.2, IF refers to the impact factor. Another approach is to define $y_{\text{Dynamic}} = (\text{DAF} - 1)y_{\text{Static}}$. Again, inserting this into Eq. 3.1 yields:

$$\text{DAF} = \frac{y_{\text{Total}}}{y_{\text{Static}}} \tag{3.3}$$

The above equation is commonly used to determine the DAF, which is the definition of dynamic allowance mostly used hereafter. Note that this definition of dynamic allowance is for a particular traffic event. For design purposes, it is important to recognise that the maximum load effect governs the design of the structure; therefore, Caprani et al. (2012) proposed using an ADR as an alternative site-specific dynamic allowance factor (see Eq. 3.4):

$$\text{ADR} = \frac{\hat{y}_{\text{Total}}}{\hat{y}_{\text{Static}}} \tag{3.4}$$

The maximum total deflection ($\hat{y}_{\text{Total}}$) and the maximum static deflection ($\hat{y}_{\text{Static}}$) are calculated for a given return period. Several authors have proposed a return period of 1000 years (with an exceedance probability of 5 % in 50 years), which accords with the definition given by EN 1991-2 (2002) for characteristic traffic loads.

3.2 Historical Review

Vibrations generated by moving loads have been studied since the collapse of the Chester railway bridge in 1847. Shortly after the accident, Willis (1849) carried out

an experiment and found that the displacement and stresses increased with vehicle speed. This work was followed by Stokes (1849), who theoretically studied the vibration of a moving mass on a massless beam. At the beginning of the nineteenth century, Kriloff (1905) and Timoshenko (1922) presented solutions for the vibration of a simply supported beam under moving loads (ML). The three most frequently used vehicle models are shown in Figure 3.1.

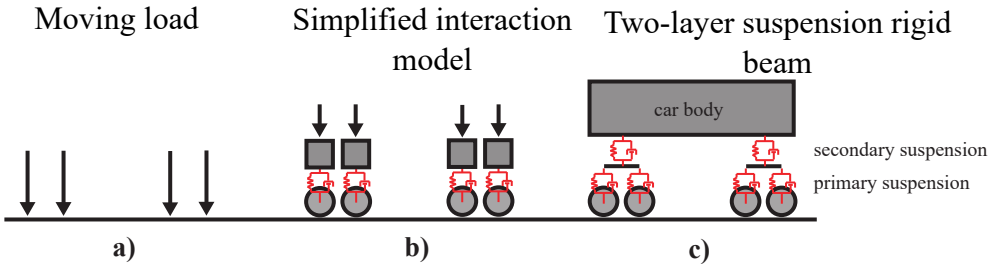

Figure 3.1: Train–bridge interaction models (Svedholm, 2017).

It was not until thirty years later that Hillerborg (1951) introduced the simplified interaction model (SIM). This is a more realistic vehicle model in which the suspension system is explicitly represented. Today, with advanced computational power, the two-layer suspension rigid beam (RB) model is the most popular VBI model. This model was used in the study by Bergenudd (2020).

Although models exist that account for VBIs, they are not used in practice. Instead, structures are designed using dynamic allowances specified by empirical equations derived from experimental results. The following section reviews the DAFs for various bridge codes.

Swedish design code

The Swedish standard for road bridges states that an impact factor $\mathrm{IF}_{\mathrm{TDOK}}$ should be added to axle and bogie loads (Trafikverket, 2020). The IF for both bending moment and shear force is provided by:

$$\mathrm{IF}_{\mathrm{TDOK}} = \frac{1.8 + 0.08\,(v - 10)}{20 + L} \leq 0.35 \tag{3.5}$$

where L [m] and $v = 80$ [km/h] are the determining length and velocity, respectively. The maximum IF is limited by 0.35. The determining length for various bridge types can be seen in Table 3.1.

Table 3.1: Determining length L according to Trafikverket (2020).

Bridge type	L
Simply supported	Span length.
Continuous	$1.2l_m$, $1.3l_m$, $1.4l_m$ and $1.5l_m$ for 2-5 span respectively ($L = 1.5l_m$ for more than 5-span). l_m is the mean span length and calculated with $l_m = \frac{1}{n}(l_1 + \cdots + l_n)$, where n are the number of spans.
Integral	Similar to continuous bridge. Frameleg should be treated as end-span.

European design code

The IF used in the European design code (EN 1991-2, 2002) is presented in ENV 1991-3 (1994). The IF has been evaluated using traffic data from different European countries. Based on the data and theoretical influences line, numerical simulations were performed, and the results were extrapolated to extreme values (an explanation of this procedure is given in Chapter 5.2 and 5.3). The results are presented in Table 3.2.

Table 3.2: Determining IF, depending on span length L [m], according to ENV 1991-3 (1994).

Section force	n-lane	IF
Moment	1-lane	$0.4 \leq 0.85 - 0.03L \leq 0.7$
Shear	1-lane	$0.2 \leq 0.45 - 0.01L \leq 0.4$
Moment & Shear	2-lane	$0.3 - 0.004L \leq 0.1$
Moment & Shear	4-lane	0.1

The IF values from the equations in Table 3.2 are included in the vehicle loads presented in EN 1991-2 (2002); however, for load model 2 and load models for fatigue an additional IF (ΔIF) should be considered. ΔIF is added to vehicle loads close to the expansion joints, and the value is calculated as follows:

$$\Delta\text{IF} = 0.3 - 1.3\frac{D}{26} \tag{3.6}$$

where D [m] is the distance from the expansion joints to the section considered. A maximum value of 6.0 m is recommended by EN 1991-2 (2002).

The AASHTO Code

The IF for the American Association of State Highway and Transportation Officials' (AASHTO's) 'Standard Specification for Highway Bridges' for 1992 was calculated based on the bridge span length according to (Deng et al., 2015):

$$\text{IF}_{\text{AASHTO}} = \frac{15.24}{L + 38.10} \leq 0.3 \tag{3.7}$$

Later, this was changed and today, according to AASHTO (2012), the IF is independent of the span length and depends on the considered components and limit states (see Table 3.3).

Table 3.3: Determining IF in accordance with AASHTO (2012).

Component	Limit state	IF
Deck joint	All	0.75
All other components	Fatigue and fracture (FF)	0.15
	All other (AO)	0.33

When existing bridges are evaluated, the IF depends on the road surface condition according to AASHTO (1989). This is further discussed and presented in Chapter 4.1.

Chinese Code

Under the Chinese code, MTPRC (1989), the IF is calculated based on the bridge span length, and it is defined according to whether the bridge is a concrete or a steel bridge. However, in 2004, a new Chinese code was introduced (MTPRC, 2004), which can be used for both concrete and steel bridges and is calculated based on the bridge fundamental frequency (Deng et al., 2015). Table 3.4 shows the different equations.

Table 3.4: Determining IF, depending on the span length L [m] and fundamental frequency of the bridge f_0 [Hz], according to MTPRC (1989) and MTPRC (2004).

Bridge type	Code	IF
Concrete	MTPRC (1989)	$0.0 \leq 0.3\,(1.125 - 0.025L) \leq 0.3$
Steel	MTPRC (1989)	$15/\,(37.5 + L)$
Both	MTPRC (2004)	$0.05 \leq 0.1767ln(f) - 0.0157 \leq 0.45$

Summary

As explained in the previous section, all design equations for determining the IF are based on empirical data. For most of these equations, the IF varies with the span length or fundamental frequency. Typically, a short bridge with a high fundamental frequency has the highest IF. The IF for various design codes is shown in Figure 3.2. To plot the curves in one graph, it is assumed that $f_0 = 82L^{-0.9}$. This equation was proposed by Tilly (1986) and has commonly been used in the literature. The figure shows that the IF varies from 0–0.8 depending on the design code and fundamental frequency. Unlike other national codes, both the Ontario Highway Bridge Design Code (OHBDC) and Swiss national codes show an increase in the IF for a frequency range of 1–6 Hz. This increased response is obtained when the fundamental frequency of a vehicle and a bridge coincide (Bergenudd, 2020).

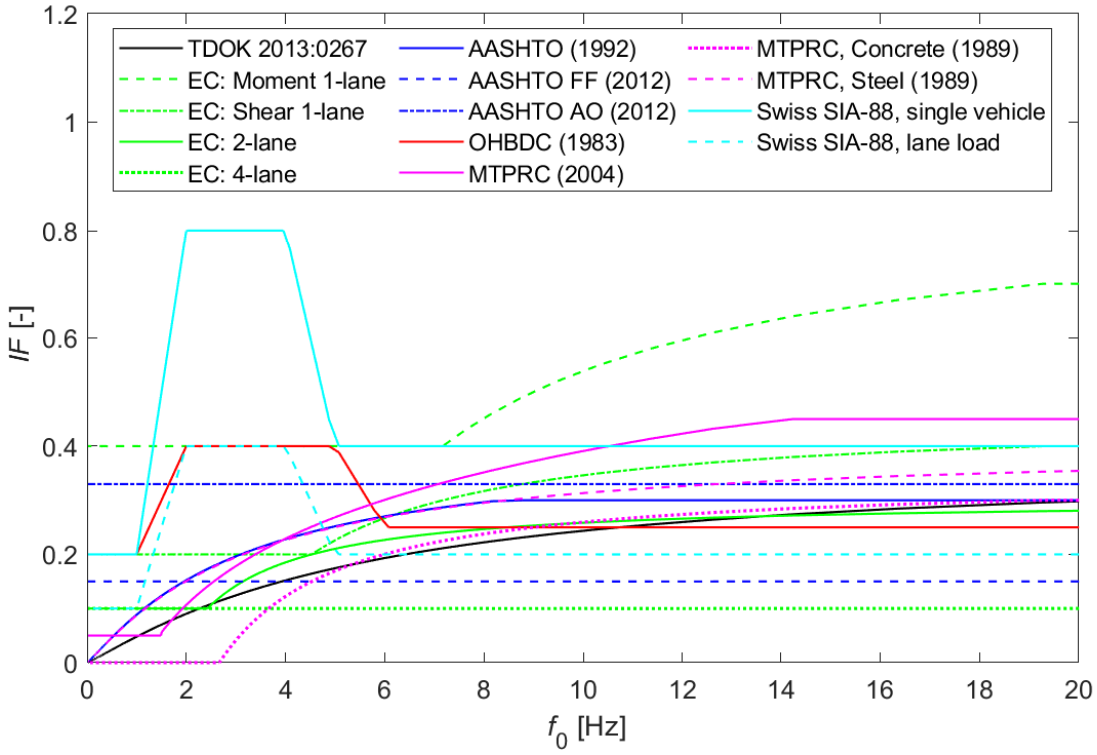

Figure 3.2: A summary of IFs based on the fundamental frequencies specified by various national codes.

4

THE MOST IMPORTANT PARAMETERS

Previous works on the area dynamic amplification for bridges, and further the DAF, have shown that many parameters affect the DAF. The parameters affecting the DAF according to McLean and Marsh (1998) are bridge fundamental frequency, bridge span, bridge damping, road irregularities, bridge type, bridge material, vehicle speed, gross vehicle weight, number of vehicles in the different lanes on the bridge, vehicle position on the bridge and vehicle suspension. The reviewed literature (Dodds, 1972; Cantieni, 1983; Billing and Green, 1984; AASHTO, 1989; Bakht and Pinjarkar, 1989; Chan and O'Connor, 1990; Hwang and Nowak, 1991; Nowak and Hong, 1991; Paultre et al., 1992; Huang et al., 1993; Nowak, 1993; Wang et al., 1993; McLean and Marsh, 1998; Scholten et al., 2004; Yang et al., 2004; SAMARIS, 2006; González et al., 2009; Ludescher and Brühwiler, 2009; Tyan et al., 2009; González et al., 2010; O'Brien et al., 2010; Cantero et al., 2011; McGetrick et al., 2013; ISO, 2016; Goenaga et al., 2017; Bergenudd, 2020; Trafikverket, 2020) shows that road irregularities, gross vehicle weight and vehicle model are the most important parameters. These parameters have a greater effect on the DAF than other parameters, and the authors believe that these are the parameters from which the industry can draw the most benefits. Some of the other parameters presented by McLean and Marsh (1998) have also been studied, along with the three most important parameters.

4.1 Road Irregularities

When a vehicle crosses a bridge, the DAF is affected by both the vehicle and the bridge itself. One parameter that has been investigated over the past few decades is road irregularities on bridges. Paultre et al. (1992) and McLean and Marsh (1998) performed extensive literature reviews on the subject in the 1990s. From analytical and experimental studies, they concluded that road irregularities had a major effect on the DAF.

Dynamic tests were performed on 226 bridges in Switzerland between 1958 and 1981 (Cantieni, 1983). The bridges were slab and beam-type highway bridges with varying total bridge lengths of 13–3147 m. The span length varied between 11 and 119 m. The effects of road irregularities were investigated by placing 40–60 mm-thick wooden planks on the bridges to represent surface irregularities. They

were placed in the traffic lane when trucks (mean gross weight of 158 kN) were crossing the bridges. The results showed a mean increase of 97.5 % for the DAF when the plank was placed on the bridge. The largest DAF was reported when the fundamental frequency of the bridge was 1.5–3 Hz or 7–15 Hz. Even if the wooden plank could represent a pothole or packed snow, the probability of having such a severe irregularity on bridges in Sweden is unlikely to occur. Conversely, Wang et al. (1993) performed a dynamic analysis of surface irregularities according to the International Organisation for Standardisation (ISO) specifications (Dodds, 1972) for very good, good, average and poor road surface. Wang et al. (1993) used a power spectrum density (PSD) function to generate road surface irregularities. The vehicle model used was H20-44 and HS20-44 trucks, as indicated in AASHTO (1989). The results of the IFs for the H20-44 truck are presented in Figure 4.1. The IF increased as the road surface became poorer, especially for average and poor road surface. An overall increase in IF can also be seen with increasing speed for good, average and poor road surface.

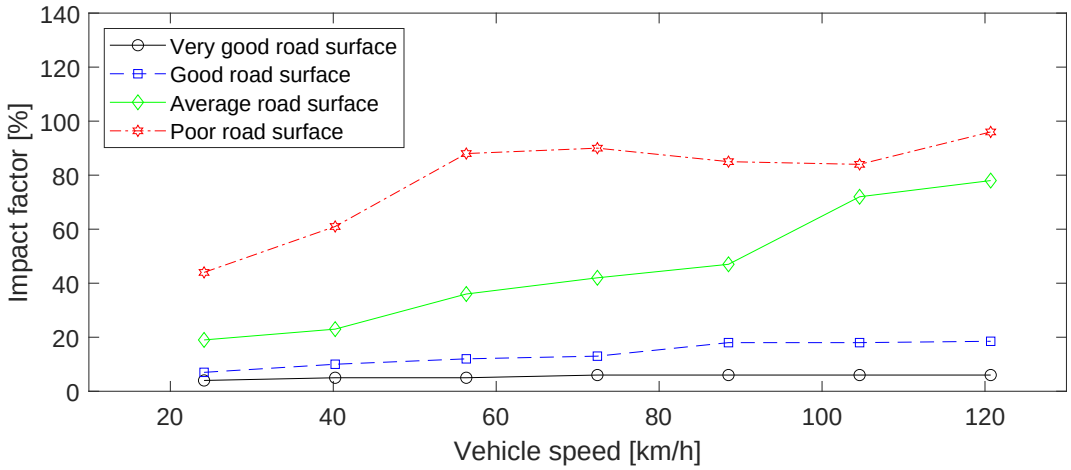

Figure 4.1: IF for the H20-44 truck depending on speed and road surface condition. Reproduced from Wang et al. (1993).

The 1989 Guide Specification for Strength Evaluation of Existing Steel and Concrete Bridges contains guidelines for assessing the load and IF of existing highway bridges in the United States (AASHTO, 1989). The static value of the load effect is scaled with an IF, which depends on the condition of the wearing surface (McLean and Marsh, 1998). IF = 0.1 is used for smooth deck conditions when no repair is needed, and IF = 0.2 is used for bridges with a rough surface (e.g. bumps and bridges in need of repair). For bridges with a span length shorter than 12 m and an extremely rough surface, a value of 0.3 should be used. In Europe, SAMARIS (SAMARIS, 2006) and ARCHES (González et al., 2009) are two projects conducted as guidance for condition assessment focusing on dynamic amplification. SAMARIS (2006) presents DAF measurements from the 'Hrastnik experiment'. A bridge with two lanes in Hrastnik, Slovenia, was selected to measure the effect on the DAF from road irregularities. The concrete bridge consisted of five simply supported spans of 30.5 m long each. The bridge was chosen because of its high dynamic response and

uneven pavement. Measurements were performed before and after resurfacing. Ruts up to 10–15 mm were found before resurfacing and the largest ruts after resurfacing were 4–5.5 mm. A total of 10770 loading events were recorded under two weeks before and after resurfacing. The highest load events recorded were higher than 700 kN in total weight. The following conclusions were obtained from the experiment:

- The average DAFs of all loading events decreased by 50 % after resurfacing.
- Using two heavy vehicles (over 380 kN total weight), the DAF was recorded as 1.050 before and 1.035 after resurfacing.
- No obvious correlation between the velocity of the vehicles and DAFs was found, inconsistent with Wang et al.'s (1993) findings.

The trend shown by SAMARIS (2006) was confirmed by González et al. (2009), who performed a dynamic simulation with a 1-dimensional model using a 5-axle truck weighing 5–65 tonne and a 10 m bridge. A total of 100 different surface profiles, also called the International Roughness Index (IRI), were used in the simulations. A higher IRI means a rougher surface and therefore more road irregularities and poorer surface condition. The results showed that the potential to obtain a higher ADR increased with an increased IRI. A low IRI had an ADR of 1.065–1.08, and a high IRI had an ADR of 1.025–1.12.

The IRI is usually modeled using a PSD function in accordance with ISO (2016) and is represented by the following spatial frequency:

$$G_d(\Omega) = G_d(\Omega_0)\left(\frac{\Omega}{\Omega_0}\right)^{-w} \tag{4.1}$$

where Ω is set to 0.01–100 rad/m, Ω_0 is the reference value 1 rad/m, and w is set to 2. ISO (2016) specifies eight road classes, A–H, with A having the lowest roughness and H having the highest. $G_d(\Omega_0)$ is set between $1{\cdot}10^{-6}$ and $1638{\cdot}10^{-6}$ m^3, depending on the road class. The displacement is represented as a function of the longitudinal distance x with an Inverse Fast Fourier Transform (IFFT):

$$r(x) = \sum_{i=1}^{N} \sqrt{G_d(\Omega_i)\frac{\Delta\Omega}{\pi}}\sin(\Omega_i x - \varphi_i) \tag{4.2}$$

where $\Delta\Omega$ is the increment between two potions, φ is a random phase shift between 0 and 2π, and N is set to the maximum number of increments (Tyan et al., 2009). Figure 4.2 shows the PSD function and road irregularities for road classes A, B and C, which represent 'very good', 'good' and 'regular', pavement conditions, respectively, according to Goenaga et al. (2017).

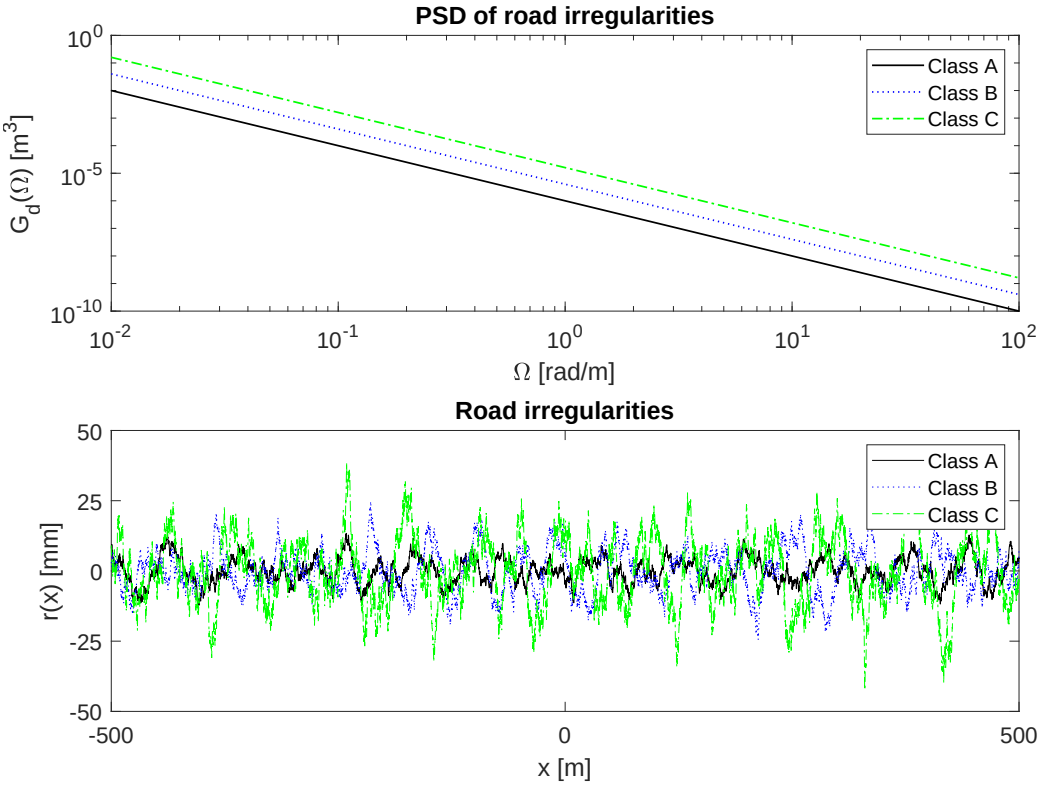

Figure 4.2: PSD of road irregularities and road irregularities for road classes A–C.

This study presents one case to visualise how the different road profiles affect deflection and further the DAF. The vehicle used is a moving 1-DOF sprung mass system (with constant speed) and a simply supported beam, which is in accordance with Yang et al. (2004) and Bergenudd (2020). The beam and vehicle properties are presented in Table 4.1. It should be noted that the beam is just a simple beam to show the trend and not a bridge-beam.

Table 4.1: Vehicle and beam properties.

Beam parameters	**Unit**	**Value**
Length	m	25
Mass	kg/m	2303
Modulus of elasticity	GPa	2.87
Area	m^2	1
Second moment of area	m^4	2.9
Damping	%	0
Vehicle parameters	**Unit**	**Value**
Sprung mass	kg	5750
Spring stiffness	kN/m	1595
Speed	km/h	100

The DAF can be calculated by comparing the static value with the dynamic values,

which were described previously in Chapter 3.1. The results from the case are presented in Figure 4.3. Deflection is shown to increase with a higher road class. Therefore, the same correlation presented in the literature can be concluded: The DAF increases with increasing road irregularities.

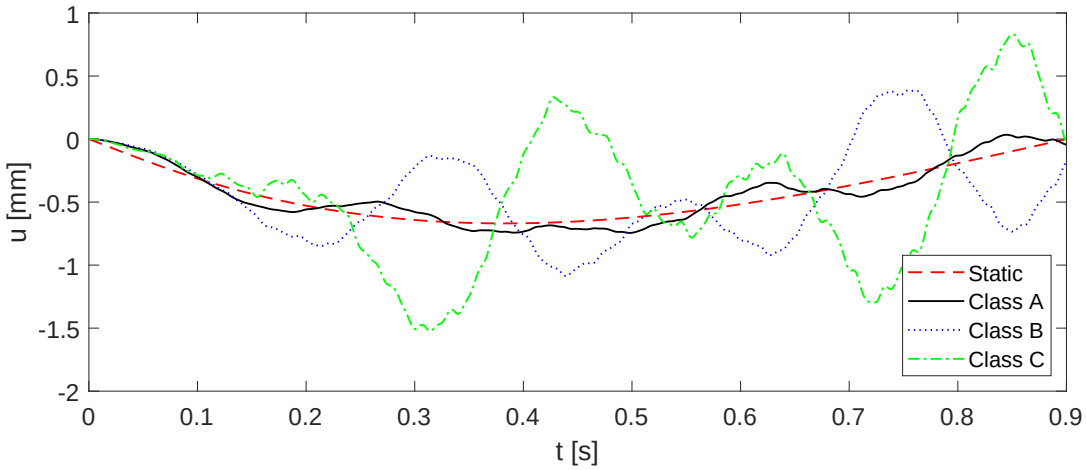

Figure 4.3: Static and dynamic deflections, depending on time, with road irregularity classes A–C when the vehicle passes over the beam.

4.2 Gross Vehicle Weight

Impact on the DAF from the gross vehicle weight (total weight from all vehicle axles) is a parameter that has received much attention from experimental and analytical investigations (Billing and Green, 1984; Chan and O'Connor, 1990; Hwang and Nowak, 1991; Huang et al., 1993; McLean and Marsh, 1998; SAMARIS, 2006; Ludescher and Brühwiler, 2009; González et al., 2009; O'Brien et al., 2010).

Experimental tests were performed on 52 bridges in the province of Ontario, Canada, from 1956 to 1957 (Billing and Green, 1984). The bridges varied in type, span length and cross-section. Over 2000 loading events were recorded, with vehicle weights varying at 50–300 kN. The overall result was unanimous: The DAF decreased with an increase in vehicle weight. At the beginning of the 1980s, additional tests were performed to determine whether the dynamic coefficients specified in the OHBDC were correct. The results showed that a reduction of the specified DAF could be made. A total of 27 different bridges were tested, and the bridge types were steel bridges (span length 22–122 m), concrete bridges (span length 16–41 m) and timber bridges (span length around 5 m). More than 100 loading events for each bridge were recorded, with vehicle weights varying at 241–580 kN. The tests in the mid-1950s showed the same trend of the DAF decreasing with increasing vehicle weight. Billing and Green (1984) reported the results from four bridges, and the decrease in mean DAF, from the lightest to the heaviest vehicles used, are as follows: 1.21–1.10, 1.20–1.07, 1.14–1.07 and 1.13–1.05. In the beginning of the 1990s, Hwang and Nowak (1991) performed analytical simulations of steel and prestressed concrete girder bridges. The bridges consisted of five girders, and the span length varied at 12–30 m. Two different trucks with varying weights were used: one three-axle single truck and one five-axle tractor-trailer. The results from the simulations are presented in Figure 4.4. The dynamic load factor decreased with an increase in the gross vehicle weight for all span lengths for both steel and prestressed concrete girder bridges. As shown in Figure 4.4, the dynamic load factor decreased more rapidly for the 12-m bridge compared with the 30-m bridge, especially for the prestressed concrete girder bridge, and the dynamic load factor were similar at higher vehicle weights for both bridges. Hwang and Nowak (1991) did also investigate the effect of varying vehicle speeds. The dynamic load factor increased for all vehicle weights up to 56 km/h, see Figure 4.4. The dynamic load factor for the vehicle weights 356 kN and 534 kN then decreased to approximately their primary values, but the dynamic load factor for vehicle weight 178 kN increased to a factor of 0.42 at 105 km/h. The overall trend is that the heaviest vehicle has the lowest dynamic load factor at different speeds.

Several authors have also reported that critical bridge loading will consist of vehicle events with multiple heavy vehicles traverse the bridge and that the DAF and ADR values decreases with multiple heavy vehicles instead of one. Hwang and Nowak (1991) reported that the DAF value decreased from 1.12 to 1.07 when two heavy vehicles were present on a 12 m-long bridge, instead of one. O'Brien et al. (2010) performed a study where characteristic loading events (generated from traffic models) were studied with a 3D bridge model and the results were analysed in terms of

ADR. It was concluded that the ADR value could be as low as 1.05, which was for one of the most critical loading events.

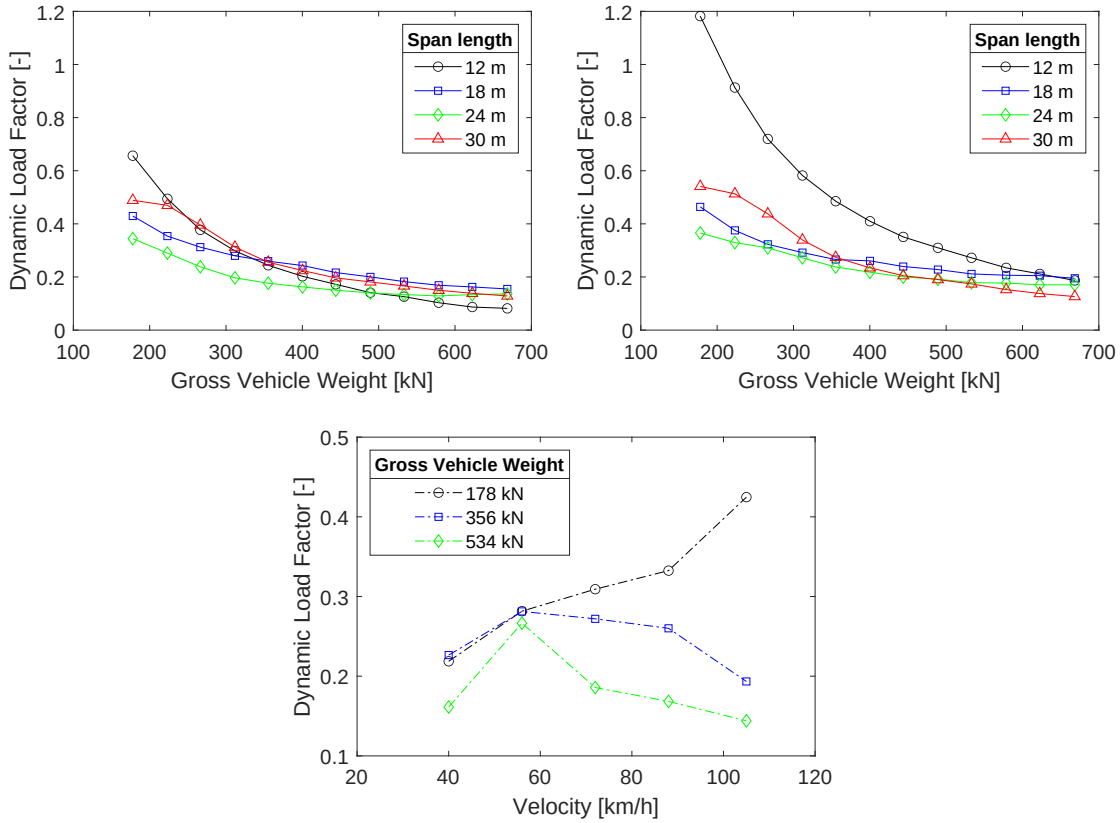

Figure 4.4: Top left: Dynamic load factor versus gross vehicle weights with varying span lengths for steel girder bridge. Top right: Dynamic load factor versus gross vehicle weights with varying span lengths for prestressed concrete girder bridge. Bottom: Dynamic load factor versus truck speed for a 30-m steel girder bridge. Reproduced from Hwang and Nowak (1991).

Another scenario is if the vehicle mass is compared with the bridge mass. As shown in Figure 4.5, the DAF increases with an increase in bridge mass compared with the vehicle mass or decreases with an increase in vehicle mass compared with the bridge mass (Ludescher and Brühwiler, 2009). McLean and Marsh (1998) explained this behaviour as follow:

> The explanation of why the impact factor decreases with heavier vehicles is that, while dynamic forces increase with increasing vehicle weight, the static load increases more rapidly with increasing weight. Thus, the impact ratio of dynamic force to live load decreases with increasing vehicle weight. (p. 22)

Note that light vehicles will result in a relatively high DAFs based on the argument above. However, the loads of light vehicles are not critical when designing a bridge. Therefore, their high DAF values are not relevant from a design perspective (Bakht and Pinjarkar, 1989). An increase in DAF also tends to occur when the vehicle

eigenfrequency and the bridge fundamental frequency are similar (Ludescher and Brühwiler, 2009).

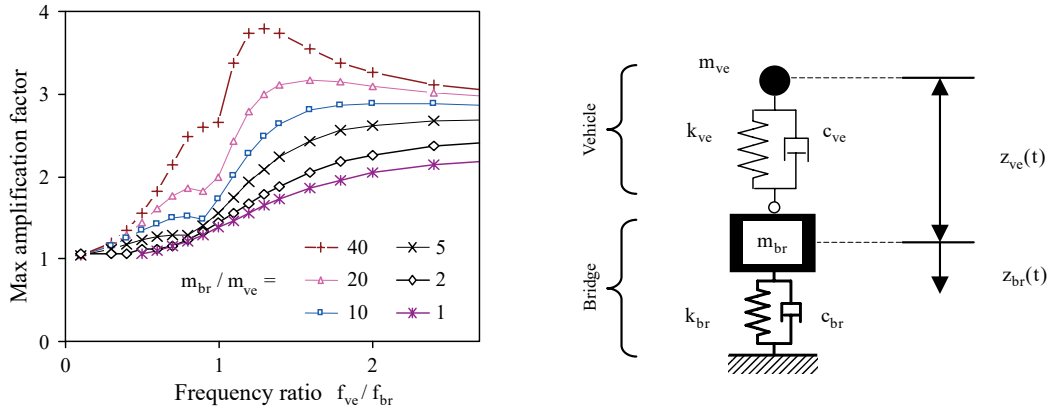

Figure 4.5: Left: Result of different bridge-to-vehicle frequency and mass ratios. Right: The used modal load model to produce the plot. Reproduced from Ludescher and Brühwiler (2009).

The trend shown by the previously mentioned authors was confirmed by the two European projects SAMARIS (SAMARIS, 2006) and ARCHES (González et al., 2009), as previously discussed in Chapter 4.1. A major objective of the 'Hrastnik experiment' in SAMARIS (2006) was to investigate the effect of increased vehicle weight on the DAF. The total weight of the vehicles passing over the bridge in the experiment was as low as 100 kN and was over 700 kN when the heaviest vehicles passed. The average DAF values from the results for different total gross vehicle weights are presented in Figure 4.6. An overall decrease in the DAF with an increase in vehicle weight is observed, especially after resurfacing of the pavement. The average DAF is as low as 1.005 at a total vehicle weight of 600 kN after resurfacing.

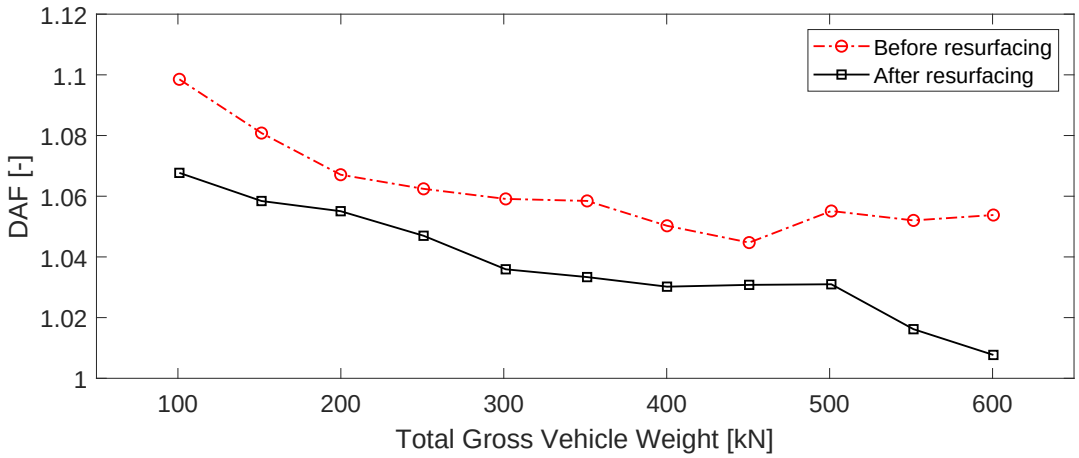

Figure 4.6: Average DAF for total gross vehicle weight before and after resurfacing of the pavement on the Hrastnik Bridge. Reproduced from SAMARIS (2006).

Analytical simulations were also executed in the SAMARIS (2006) project. The results from the simulations supported the results from the experimental tests on Hrastnik Bridge. In general, real DAF values are lower than those presented in relevant design codes, especially in higher loading events on the investigated bridges (SAMARIS, 2006; González et al., 2009). However, there is one design code that follows the presented trend. The guideline document called Reliability-Based Classification of the Load Carrying Capacity of Existing Bridges (Scholten et al., 2004) was published by the Danish Road Directorate in 2004. It is used in Denmark when a traditional deterministic classification of an existing bridge does not provide the required results. Scholten et al. (2004) presented a dynamic factor for global effects (influence length ≥ 2.5 m), which was calculated based on an independent normally distributed variable: $N(41.5/W;\ 41.5/W)$, where W is the total vehicle weight in kN for the individual vehicle. Figure 4.7 shows the DAF recommended by Scholten et al. (2004) with varying gross vehicle weights. A clear reduction in the DAF is observed when the gross vehicle weight increases.

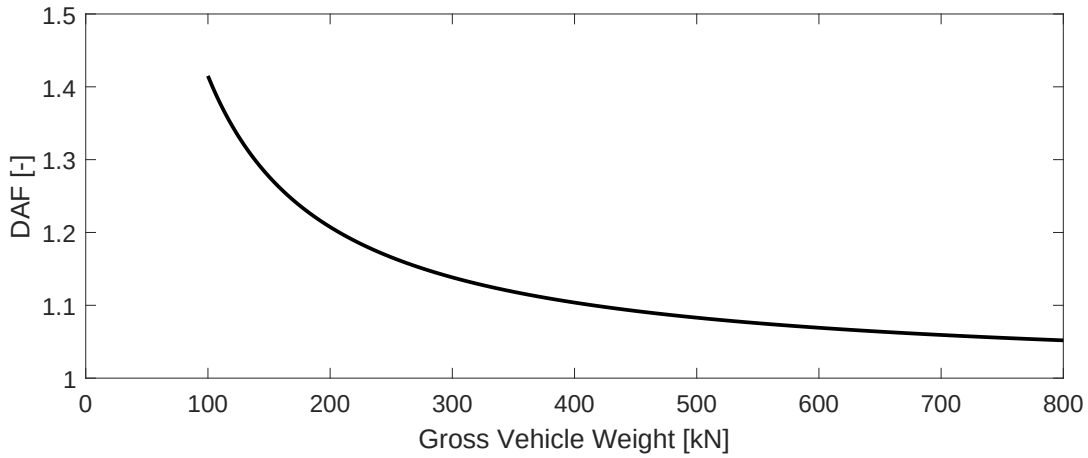

Figure 4.7: Recommended DAF with varying gross vehicle weights (Scholten et al., 2004).

SAMARIS (2006) reported the recorded DAF for each vehicle event on Hrastnik Bridge, which is visualised in Figure 4.8. The Danish reliability-based bridge assessment (RBBA) code (Scholten et al., 2004) is also presented in the figure. The RBBA code follows the trend with a decreased DAF at higher vehicle weights. Some of the recorded DAF values are greater than the RBBA code, but, as Bakht and Pinjarkar (1989) stated, the loads of light vehicles are not critical for the design. A load-carrying capacity assessment of Hrastnik Bridge with the RBBA code follows the DAFs of the largest loads, which probably would be the critical loads for the capacity. The RBBA code is compared with the Swedish DAF and calculated using Eq. 2.1, as presented in Chapter 2.1, and is in accordance with TDOK 2013:0267 (Trafikverket, 2020). At the largest loading event at 719 kN, the Swedish DAF is higher than the DAF from the RBBA code. Specifically, the Swedish DAF is 5.1 % higher than the RBBA code at 719 kN. This will result in a 5.1 % higher load effect if a load-carrying capacity assessment is performed with the Swedish DAF instead of the Danish DAF.

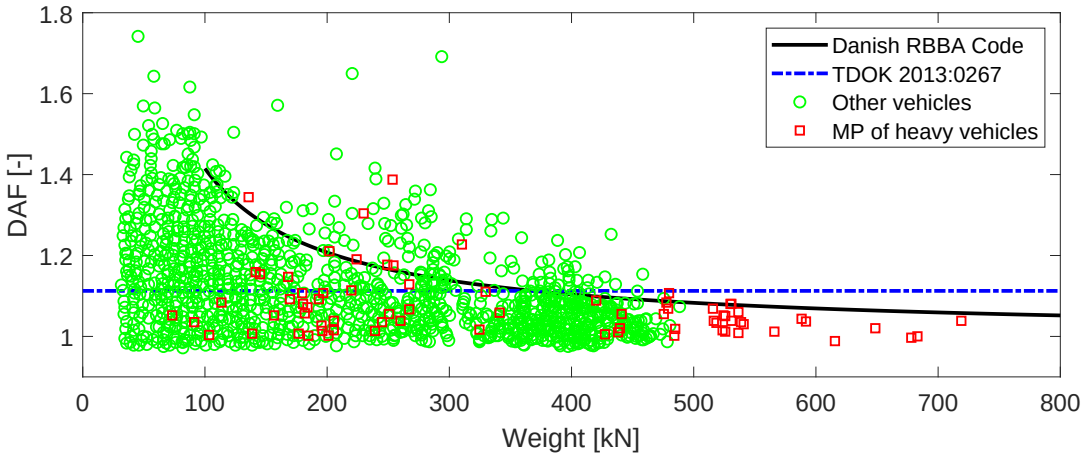

Figure 4.8: Recorded DAF after resurfacing of the pavement on Hrastnik Bridge for loading events with multiple presence (MP) of heavy vehicles and other vehicle events compared with TDOK 2013:0267 (Trafikverket, 2020) and the Danish RBBA code (Scholten et al., 2004). Reproduced from SAMARIS (2006).

DAF versus strain measurements were performed on five bridges in the ARCHES project (González et al., 2009). The bridges were of different types, and the span lengths varied between them. One of the five bridges is Trebnje Bridge, an 11.65 m integral reinforced concrete slab bridge. A total of 56475 loading events were recorded over a period of 33 days. The DAF value at the highest strain was 1.015, see Figure 4.9. Another bridge that was included was the Ivanje selo viaduct, a 225-m-long 9-span viaduct with 7 prefabricated 25.0-m-long simply supported prestressed concrete beams. The deck is a continuous cast-in-place deck of reinforced concrete. A total of 121000 loading events were recorded over a period of 60 days. The highest strain was caused by a loading event with a DAF value of 1.005, which is presented in Figure 4.9. As shown in Figure 4.9, the DAF decreases with an increase in the average static strain. The recorded values are consistent with the Danish RBBA code, especially at higher strain values. As presented in Figure 4.8, the Swedish DAF is higher than the Danish DAF at higher strain/weight values. However, the difference between them is larger at Trebnje Bridge than at the Ivanje selo viaduct. The difference is due to the different span lengths between the bridges. The only unknown variable in the equation used to calculate the Swedish DAF (Eq. 2.1) is the span length. A shorter span length results in a higher DAF. As long as the influence length is equal to or longer than 2.5 m, the RBBA code will result in the same DAF. The results for Trebnje Bridge in Figure 4.9 show that the Danish DAF at the highest measured strain is equal to 1.041 and that the Swedish DAF is 1.256. The RBBA code overestimates the real DAF by only 2.6 %, but the Swedish DAF overestimates the real DAF by 23.7 %. This means that a load-carrying capacity assessment performed with the Swedish DAF would result in a 20.6 % higher load effect than that performed with the Danish DAF.

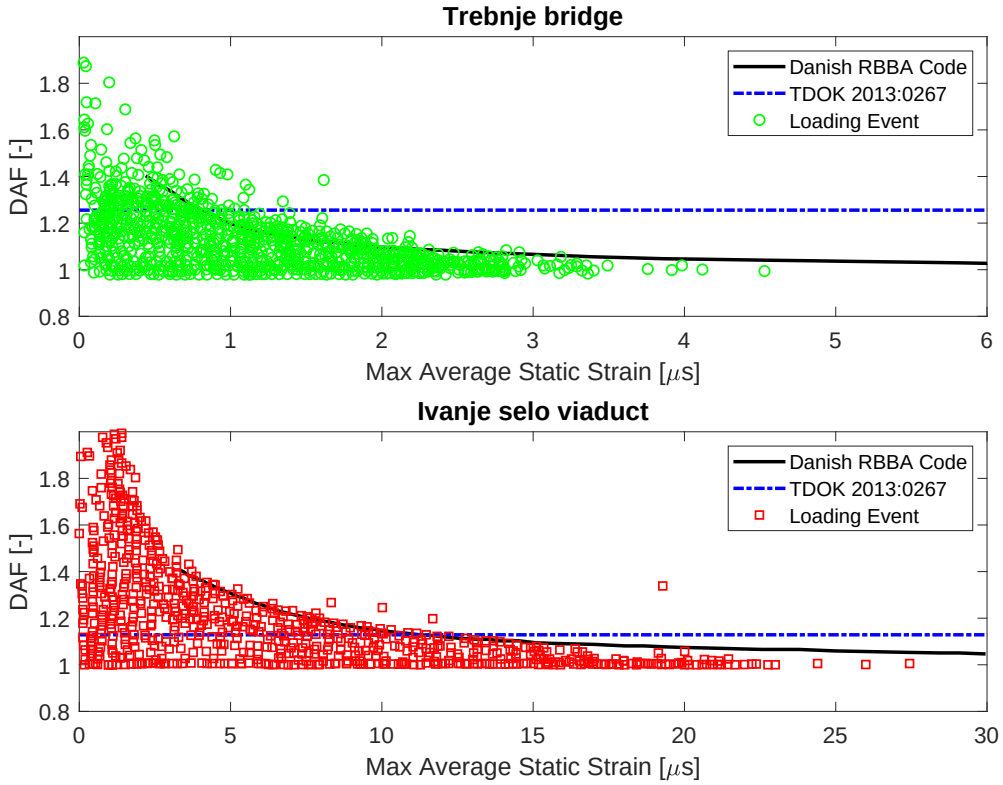

Figure 4.9: Results of the DAF–Strain measurements from the Trebnje Bridge and the Ivanje selo viaduct. The Danish RBBA code (Scholten et al., 2004) compared with TDOK 2013:0267 (Trafikverket, 2020). Reproduced from González et al. (2009).

The literature shows a clear trend: An increase in gross vehicle weight results in a decreased DAF. Three examples from the experimental tests show that the Swedish DAF overestimates the real DAF at larger vehicle weights and higher strain values, which usually determine the design. The DAF presented by the Danish RBBA code (Scholten et al., 2004) tends to fit the trend better.

4.3 Vehicle Model

Results from analytical and experimental investigations were presented in previous chapters. The advantage of analytical investigations is that no or just a small amount of field data needs to be collected. It can take years or decades to obtain a sufficient amount of data just by collecting it in the field (González et al., 2009). Using simulations with numerical VBI models dramatically decreases the investigation time, and such models have been used by many authors in the literature (Nowak and Hong, 1991; Paultre et al., 1992; Huang et al., 1993; Nowak, 1993; Wang et al., 1993; McLean and Marsh, 1998; SAMARIS, 2006; González et al., 2009; Ludescher and Brühwiler, 2009; González et al., 2010; Cantero et al., 2010; O'Brien et al., 2010; Cantero et al., 2011; McGetrick et al., 2013; Bergenudd, 2020). One decisive aspect when conducting an analytical experiment is to model the vehicle and its behaviour as similar to real vehicles as possible.

Bergenudd (2020) examined different types of vehicle models. Figure 4.10 shows one of the vehicle models called Truck 2, which was also used by González et al. (2010) and McGetrick et al. (2013). The vehicle consists of a rigid body with front and rear axle. The rigid body is characterised by mass, m_S, and rotational moment of inertia, I_S, and has two motions: vertical translation, y_S, and pitch, θ_S. The body is connected to suspension units. The suspension and tires are modeled as spring-dashpot units with stiffness, $k_{s,i}$ and $k_{t,i}$, and viscous damping, $c_{s,i}$ and $c_{t,i}$. The axle and wheel mass are joined together, m_i, and have a vertical translation, y_i.

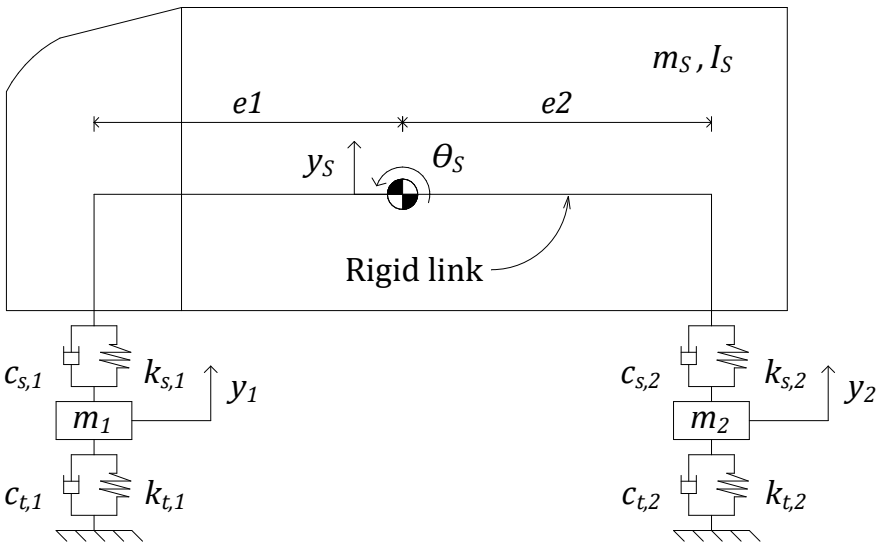

Figure 4.10: Vehicle model Truck 2 with a rigid link, which symbolises the connection between the suspension units and the truck body. From Bergenudd (2020).

Regular light trucks have frequencies of 1–3 Hz, and heavy trucks have frequencies of 2–5 Hz (González et al., 2010). Heavy trucks tend to have two vibrational modes: 2–5 Hz is caused by body bounce and 10–15 Hz by tire hop (McLean and Marsh,

1998). According to Ludescher and Brühwiler (2009) are the frequencies for body bounce, or pitching, between 1.5 and 4 Hz. The values for body bounce (Modes 1 and 2) and tire hop (Modes 3 and 4) for Truck 2 are presented in Figure 4.11. Truck 2 has lower values than the values reported by McLean and Marsh (1998). Paultre et al. (1992) supports the values for tire hop at 10–15 Hz but reported that it has a low influence on the DAF for bridges. The frequency caused by body bounce or pitch tends to be at the interval where the DAF is most affected. The highest DAF is created when bridges have a fundamental frequency of 2–5 Hz (McLean and Marsh, 1998). As discussed in Chapter 4.2 (see Figure 4.5), the DAF increases when the vehicle eigenfrequency and the bridge fundamental frequency are similar. The suspension is the vehicle component that controls body bounce or pitching.

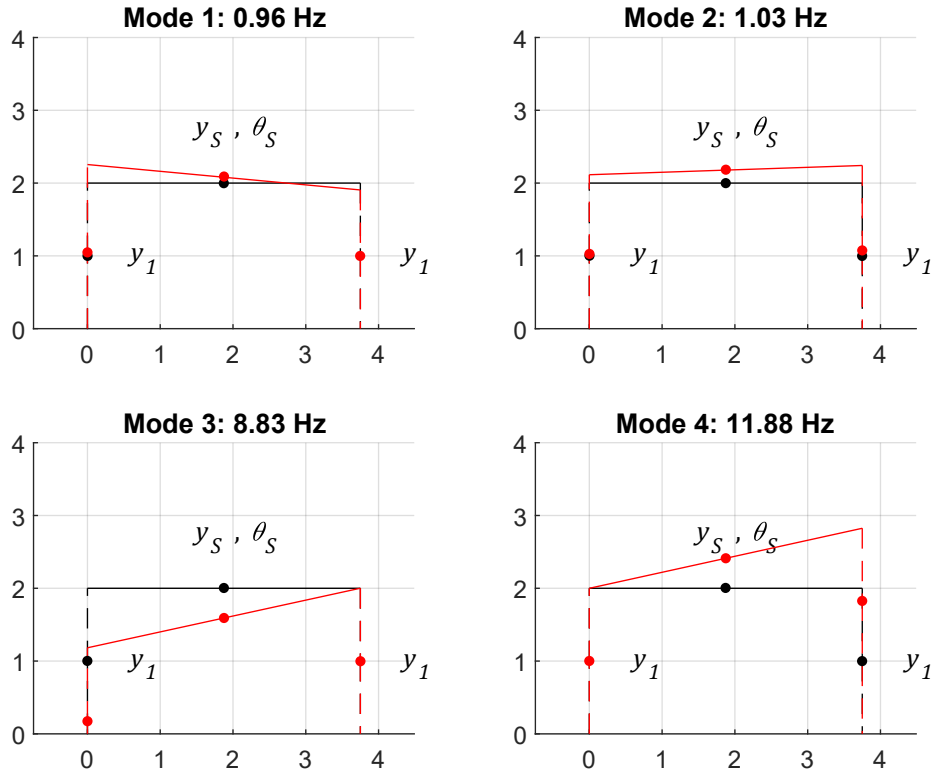

Figure 4.11: Eigenmodes for Truck 2 with air suspension. Mode 1: suspension pitch mode. Mode 2: suspension hop mode. Mode 3: tire pitch mode. Mode 4: tire hop mode. From Bergenudd (2020).

There exist more complex models than the one presented in Figure 4.10. González (2001) and Cantero et al. (2010) presents 3D VBI models that can include articulations, trailers or axle groups. The advantage with 3D models instead of 2D is that results with higher accuracy can be obtained (González et al., 2009). Other advantages are that individual road profile for each wheel path or different suspension stiffness for all wheels can be used.

There are two types of suspensions: air and steel leaf suspension. Studies (McLean and Marsh, 1998; Cantero et al., 2011; González et al., 2010; Ludescher and Brüh-

wiler, 2009; Bergenudd, 2020) have shown that the use of air suspension results in a lower DAF than compared with a steel leaf suspension. Air suspension has a softer characteristic and is not as stiff as leaf suspension. Cantero et al. (2011) performed an analytical study on two heavy vehicles: a 5-axle truck and a large mobile crane. The results show that stiffer suspension leads to a higher probability of obtaining a higher DAF, see Figure 4.12. The vehicles passed bridges with varied span lengths of 7.5, 15, 25 and 35 m. The larger DAF values for leaf suspension compared with air suspension at low bridge frequencies are assumed to correspond to the lower suspension modes (Bergenudd, 2020).

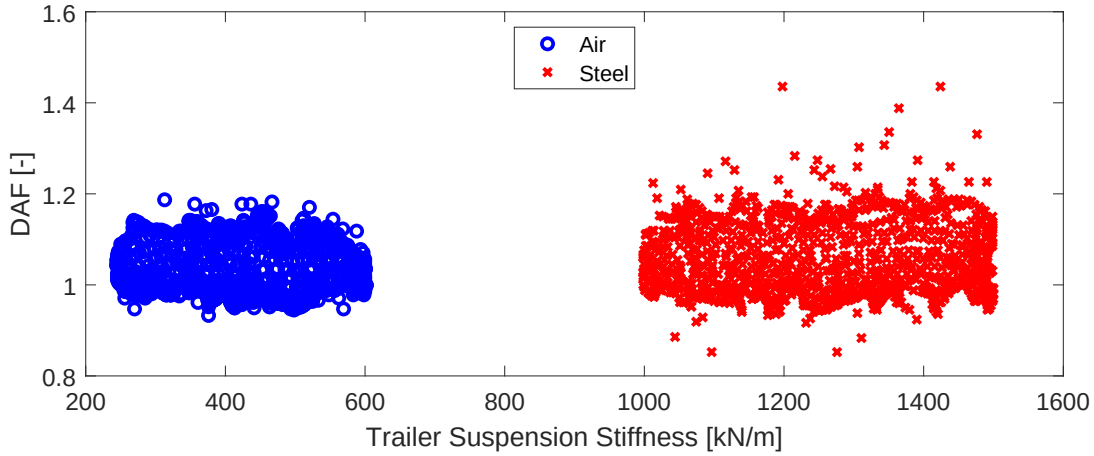

Figure 4.12: Air versus steel leaf suspension. Reproduced from Cantero et al. (2011).

5

SITE–SPECIFIC DYNAMIC ALLOWANCE

When performing a traditional bridge assessment, predefined traffic load values and their dynamic effects are used based on standards that need to cover many different traffic situations; thus, conservative values are used (O'Brien and Caprani, 2005; SAMARIS, 2006; González et al., 2009; Caprani et al., 2012; Caprani, 2013; Carey et al., 2017). Traffic loads and dynamic amplifications are the most variable parameters when a bridge assessment is performed (Caprani et al., 2012). Using site-specific information often results in lower dynamic amplifications and, consequently, more accurate assessments, compared with assessments performed with predefined values based on standards (SAMARIS, 2006; González et al., 2009). This section explains how site-specific information can be collected and used to evaluate site-specific dynamic allowances for designs, also called ADR. It also presents methodologies for both experimental measurement and numeric models.

5.1 Weigh-In-Motion Systems

To investigate dynamic amplification, it is of great benefit to collect site-specific data. One technique used in the reviewed literature (Hwang and Nowak, 1991; Nowak and Hong, 1991; Nowak, 1993; DIVINE, 1998; Vägverket, 2004, 2006; SAMARIS, 2006; Carlsson and Karoumi, 2008; González et al., 2009, 2010; Cantero et al., 2011; Caprani et al., 2012; O'Brien et al., 2012; Malekjafarian, 2016; Carey et al., 2017; Bergenudd, 2020) to collect information about vehicles and their impact on bridges is weigh-in-motion (WIM) systems. WIM systems have been used since the 1970s and have developed over the years (Vägverket, 2004).

In the mid-1980s, Sweden used fixed weigh stations, but due to their high cost and poor results, they were not ideal (Vägverket, 2004; Carlsson and Karoumi, 2008). A WIM system that has been used instead in later years is the portable bridge weigh-in-motion (BWIM) system, which is used to measure traffic flows at normal speed and register axle spacing, loads, number of axles per vehicle, gross weight, speed, and vehicle class (Vägverket, 2004; SAMARIS, 2006; González et al., 2009). In recent years, the system has been developed to record data for use in evaluating bridges with normal traffic. Measurements were previously statically executed with pre-weighed vehicles. Structural data such as influence lines, statistical load distributions, and IFs can now be evaluated without the need to close bridges (SAMARIS, 2006),

since data is collected from vehicles that pass over bridges daily. An upgraded BWIM system called SiWIM has been used by several authors (Vägverket, 2004, 2006; Carlsson and Karoumi, 2008; SAMARIS, 2006; González et al., 2009). One advantage of SiWIM is that it uses real influence lines from bridge data, rather than the theoretical influence lines used by older BWIM systems (González et al., 2009). The installation on a bridge is described in Figure 5.1. Axle detectors are placed on a bridge, and strain gauges are located under the bridge. The signals are passed to a computer, which sends the data to the user. González et al. (2009) reported that, traditionally, axle detectors on bridges are at risk of damage due to the impact of vehicles. Nowadays, with the SiWIM system, is it more common to use free-of-axle detector (FAD), also known as NOR (nothing-on-the-road). With FAD, additional strain transducers are placed at the same spacing distance as axle detectors, but under the bridge (Žnidarič et al., 2005); thus, all the equipment is protected from vehicles passing over the bridge. The system needs to be calibrated before it can be used. A pre-weighed vehicle is used to correlate the recorded strains with the actual vehicle weight (Vägverket, 2004; SAMARIS, 2006; González et al., 2009).

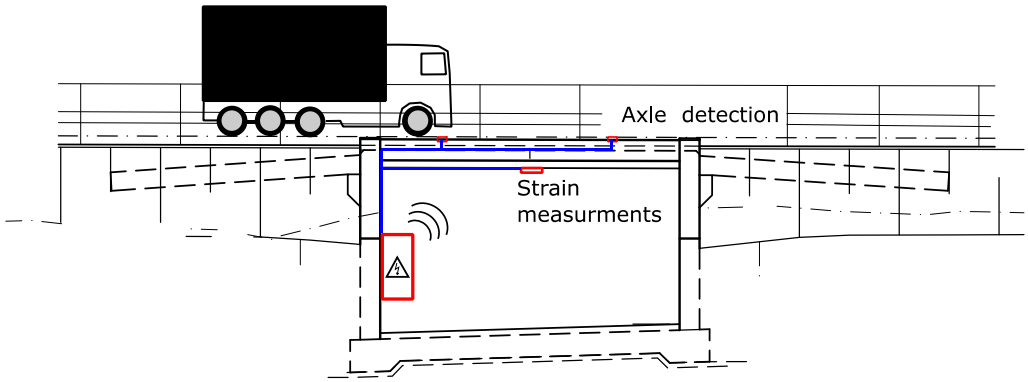

Figure 5.1: Concept of the installation of a SiWIM.

New BWIM systems can also detect the transverse positions of vehicles and their axles. This was an important factor when the Ölandsbron load-carrying capacity assessment was performed by Carlsson and Karoumi (2008), since the Ölandsbron is a beam bridge with cantilever slabs on the edges. The measurements showed that the vehicles tended not to drive as close to the edge of the bridge as first assumed in the calculations, which was favourable for the load-carrying capacity assessment.

Even though today's BWIM systems are portable, they still need to be mounted, reinstalled, and recalibrated for monitoring of a new bridge. Instrumented vehicles with on-board weighing (OBW) systems are now being developed. An OBW system measures vehicles' gross and/or axle weights and can be used for different types of vehicles (Radoičić et al., 2016; Patel and Vinay, 2020; Zhang et al., 2021) and different heavy industries (e.g. mining and construction) to monitor the weight of vehicles' cargos. This is important because heavy loads can damage vehicles (Radoičić et al., 2016). Studies have also reported that the heavy transportation industries in Europe and Sweden sometimes exceed the limits for gross vehicle and/or axle weight (Vägverket, 2004, 2006; Lydon et al., 2014). This results in wear and tear

on roads and bridges, which further results in negative environmental and economic effects. Zhang et al. (2021) presented an OBW system for weighing the cargo on trucks. Strain sensors (gauges) are attached to the frames of vehicles, which calculate the loads and send the values to on-board computers. The system is driven by the battery in the vehicle. This kind of system can be used to monitor traffic flows and evaluate the structural data of bridges (see Figure 5.2). If an OBW system is used in a vehicle, there is no need for axle detection on bridges. The weight of a vehicle is measured by the OBW system, and the location of the vehicle can be tracked with GPS, making it possible to see which bridge the vehicle is passing over. Only strain gauges need to be installed on bridges to evaluate vehicles' impacts on the bridges. The data from the vehicle and the equipment on the bridge are sent automatically to the user.

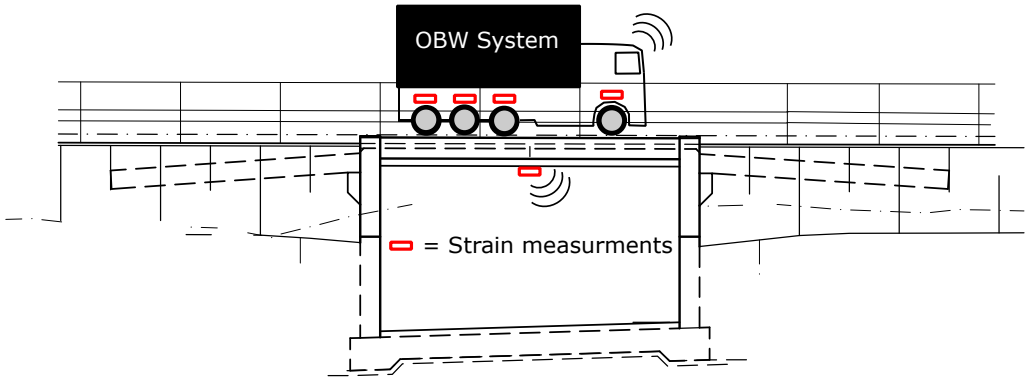

Figure 5.2: Concept of an OBW system with on-bridge strain measurements.

Accelerometers are another component of OBW systems. González et al. (2010) and Malekjafarian (2016) presented a method in which accelerometers are attached to a vehicle's axles. With accelerometers, bridge dynamic properties such as natural frequency, damping, and mode shapes can be measured when a vehicle passes over a bridge. The idea is to detect whether some of the bridge's dynamic parameters are changing over time, enabling bridge structural conditions to be monitored. The advantages of this method are that no equipment needs to be attached to bridges and that many bridges can be monitored in a short period. The disadvantages are that this technique has been shown to be sensitive to vehicle speed and road profile, resulting in difficulties in obtaining reliable results.

5.2 Experimental Measurement

Experimental measurement is one method of obtaining DAF results and further value for bridge design, based on ADRs (Chapter 3.1). In Chapter 4, most of the results are presented with DAF values, but as previously explained in Chapter 3.1, this is only for specific traffic events. Some authors have presented the results of their studies using ADR values instead, which can be used for bridge assessment over a determined return period. Figure 5.3 presents a methodology and workflow for experimental measurements proposed by González et al. (2009), O'Brien et al. (2012), and Carey et al. (2017), with the aim of obtaining ADR values for bridges.

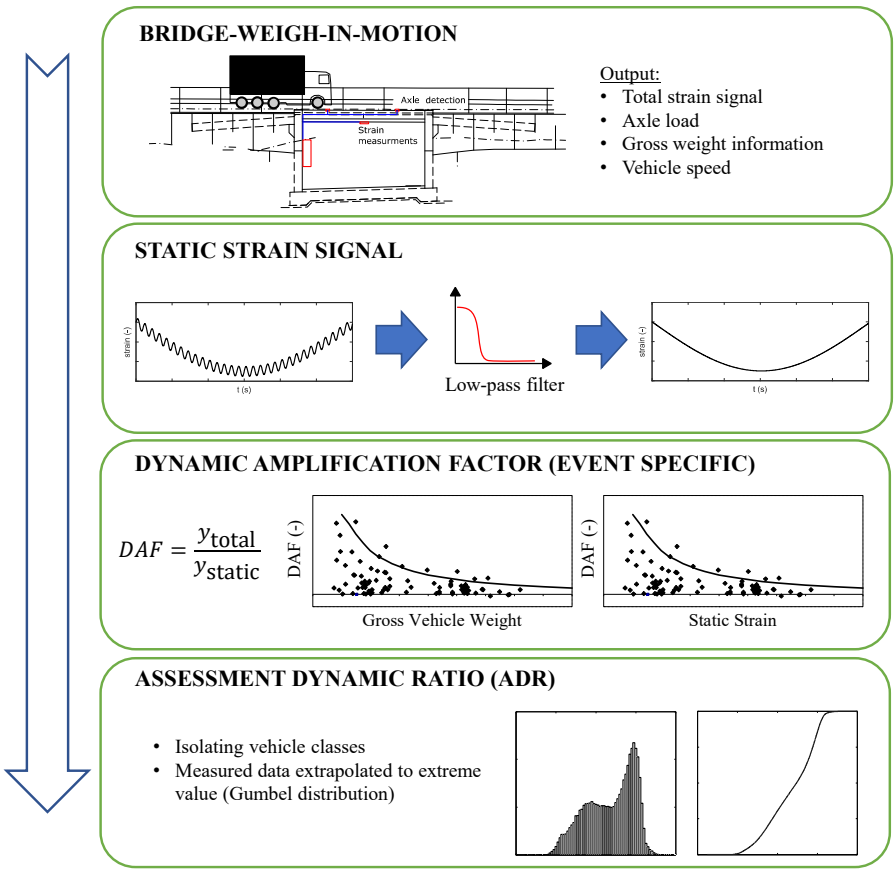

Figure 5.3: Methodology proposed for experimental measurements.

Each step of the workflow (Figure 5.3) is explained in more detail in the following sections.

BWIM. The first step of experimental measurement is to collect data from the site. To evaluate the impact of vehicles on the bridge of interest, information as strain, axle load weight, and speed needs to be assembled. Different techniques for collecting the information were presented in the previous chapter (Chapter 5.1), of which the most frequently used is the SiWIM system.

Static Strain Signal. When the data is obtained, some information needs to be separated, which can be done using different filtering techniques (Žnidarič et al., 2008; Žnidarič and Lavrič, 2010). The use of a low-pass filter makes it possible to separate the static strain from the total strain (Žnidarič et al., 2008), in turn making it possible to calculate the DAF. This technique was used by the ARCHES project (González et al., 2009), and the WIM system was used to relate each calculated DAF to the vehicle's gross weight and the category of the vehicle (e.g. the number of axles and spacing). Filter techniques can also be used for other purposes. González et al. (2009) filtered WIM data to only show data from specific types of vehicles, and Carey et al. (2017) used a filter technique to find influence lines.

DAF. The DAF is calculated for each loading event during the time the bridge is monitored. It is important that every DAF value can be related to a vehicle's gross weight and category. Most of the authors in Chapter 4 presented DAFs for gross vehicle weight, but González et al. (2009) presented them for static strain. There are also differences in how the strains are evaluated. In the SAMARIS project (SAMARIS, 2006), the SiWIM was used with an algorithm that calculated the DAF directly. SAMARIS (2006) compared the measured total strain response with the theoretical static strain response. The theoretical response was calculated using influence lines multiplied by weighed axle loads from the BWIM system. This system requires high weighing accuracy. Even if axle loads were correctly evaluated, it was shown that some errors occurred in velocity measurement and some axles were not accurately classified. This resulted in incorrect static signals, which further resulted in outliers, requiring manual work to be done (González et al., 2009; Žnidarič and Lavrič, 2010). Due to the sensitivity, it is better to use the low-pass filter presented above than to calculate the DAF.

ADR. As shown in Chapter 4, the vehicles that result in the highest DAFs are not the ones that contribute to the greatest strains or the heaviest load effects; therefore, it is important to know the DAF, gross weight, strain, and vehicle category for each loading event to calculate an ADR value. González et al. (2009) calculated a site-specific ADR for each of three bridges in the ARCHES project for which experimental measurements had been performed. Each ADR value was calculated for a return period of 1000 years, in line with EN 1991-2 (2002), to determine characteristic traffic load. Initially, all the data for the DAF–strain results was plotted on Gumbel probability paper for total and static strain. The plots did not show any strong correlations, making it difficult to extrapolate to extreme values. One explanation for this was that the data included all vehicle classes. González et al. (2009) then isolated vehicle classes and plotted the data as histograms to find a reasonable DAF trend and further ADRs. When the vehicle classes were isolated and the mean and standard deviation were known, it was possible to extrapolate to extreme values and produce Gumbel distributions with reliable results. Carey et al. (2017) used a similar method for experimental measurements performed over 45 days on an 18.8 m-long beam-and-slab bridge with 27 prestressed concrete girders in Ireland. Carey et al. (2017) isolated the characteristic strain values that had a 99.9 % probability of non-exceedance (i.e. the 0.1 % of vehicle events with the highest strain values).

These strain values corresponded to the heaviest trucks, and an ADR value was calculated based on the data.

Based on the findings above, it is beneficial for vehicle classes to be isolated and the data within each class extrapolated to extreme values.

5.3 Numerical Models

Even if measured load effects from experimental measurements do not exist, it is still possible to perform site-specific bridge assessments. By using some site-specific input and numerical models, ADR design values can be calculated. Figure 5.4 presents a methodology and workflow for numerical models proposed by González et al. (2009), O'Brien et al. (2010), Caprani et al. (2012), and Caprani (2013). This section will mainly present this methodology for the calculation of an ADR value for the Mura River Bridge, which was performed by González et al. (2009) and later summarised and evaluated by Caprani et al. (2012). The bridge, located in Slovenia, is a multiple-span bridge, but the investigated part was a 32-m-long simply supported bridge span. The bridge is a beam bridge with five prestressed concrete beams and a reinforced concrete slab. It has two traffic lanes, one in each direction.

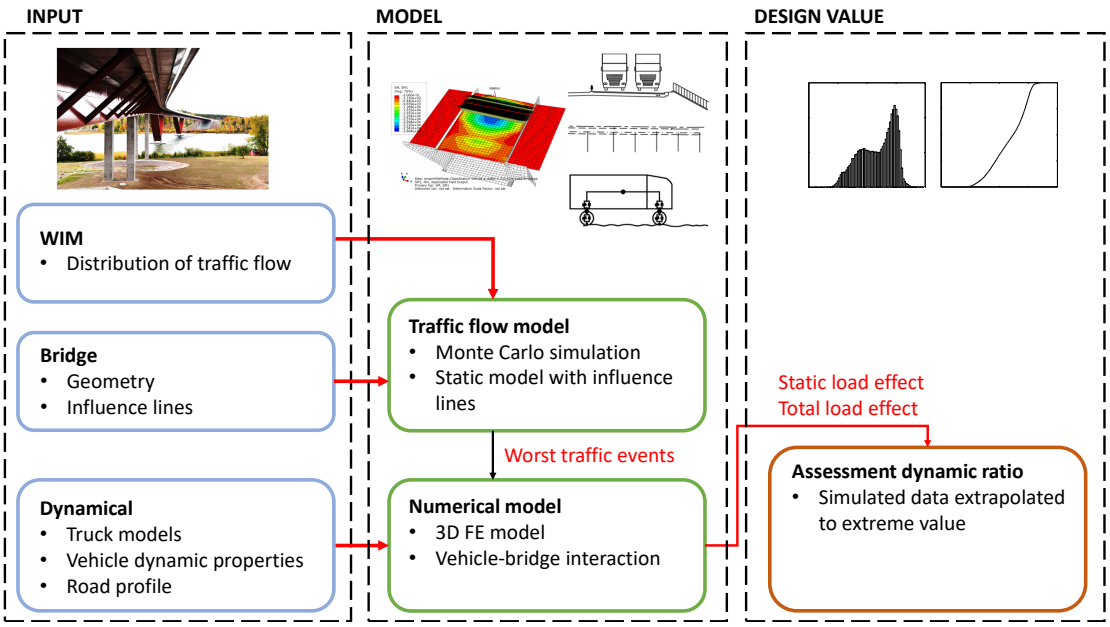

Figure 5.4: Methodology proposed for numerical models.

The first step in performing a site-specific bridge assessment with numerical models is to collect the needed input data. One input is the traffic flow and information about the vehicles, such as the vehicle gross and axle weights, spacing between the axles, speed, and which traffic lane the vehicles are travelling in. This data can be collected using a WIM system (Chapter 5.1). Information about the bridge, such as the geometry and influence lines, must be known. Different truck models and their dynamic properties (Chapter 4.3) are other parameters to be considered. Road profile can be measured on the site as in the SAMARIS project (SAMARIS, 2006) or using predefined values from ISO (2016), see Chapter 4.1.

The largest difference between experimental measurements and numerical models is how the static and total load effects are obtained. The key purpose of numerical models is to model the traffic as identical to the real traffic to find the worst traffic

events and load effects. The section below explains how this can be done effectively.

Traffic flow model. When the input data is collected, it is possible to develop a model, but the vehicle data must first be known, and it is not clear how vehicles are passing over the bridge. Information such as the distance between the vehicles and different configurations of vehicle categories on the bridge in different traffic lanes is also unknown. Different configurations could be investigated directly with a VBI model, but this would require excessive computation time. Instead, Caprani et al. (2012) first used a statistical Monte Carlo simulation, developed by O'Brien and Caprani (2005), to produce a traffic flow model with minimal computation time. O'Brien and Caprani (2005) used the data from WIM measurements and noted the mean traffic flow per hour. Cumulative distribution functions were calculated based on the flow rate. Simulations were performed with different configurations of vehicles on both traffic lanes to find the worst loading events along the defined influence lines. One key parameter to consider is the gap between the vehicles (also known as headway). The headway is defined as the distance or time between a vehicle's rear axle and the front axle of the vehicle behind. Different distribution functions with different headways were investigated to find the worst scenarios. The Monte Carlo simulations generated data for bi-directional free-flowing traffic over a period of ten years to determine the 100 events that created the maximum static load effects. The events consisted of 20 one-truck events, 77 two-truck events, and 3 three-truck events.

Numerical model. The 100 worst loading events from the static evaluation were further used to examine the total load effects. The bridge model was used to define the influence lines for the static evaluation of the load effects, as previously presented. Instead of using a simplified 2D model González et al. (2009) used the 3D VBI FE model from González (2001) (mentioned in Chapter 4.3) together with a 3D FE bridge model to obtain highly accurate results. The two- and three-axle vehicles were modelled as rigid body vehicles, and the four- and five-axle vehicles were modelled as articulated vehicles. The simulations for the FE models enabled the total load effects to be known for the 100 worst loading events, and the DAF and ADR values could then be calculated.

An ADR value was calculated as presented in Chapter 5.2. First, a Gumbel bivariate extreme value distribution was used to model the total and static load effects, and then a parametric boot-strapping method was used to produce extreme values and obtain a further design value that represented an ADR value for a design lifetime of 100 years. The result was a value of 1.06 (Caprani et al., 2012), which is comparable with the value of 1.14 if the Swedish norm Trafikverket (2020) would be used.

In another study, Caprani (2013) proposed not only including free-flowing traffic load models in simulations but also using traffic congestion load models. Investigations have shown that the worst traffic events, for short- to medium-length bridges, can be caused by traffic congestion. According to Caprani (2012), drivers' behaviour changes in traffic congestion situations compared with their behaviour under free-

flow traffic conditions. This results in different assumptions regarding the headway, meaning that different models must be used. Therefore, Caprani (2013) produced a general extreme-value theory model that included both a free-flowing traffic model (O'Brien and Caprani, 2005) and a congested-flow traffic model (Caprani, 2012).

Lastly, the condition of a bridge varies during its lifetime. When performing experimental measurements, load effects are evaluated based on the condition of the bridge during that time. One advantage of numerical models is that variations can be simulated; for example, a changed road profile and bumps on or before the bridge can cause increased dynamic amplification, but this can be evaluated during investigations and taken into account when an ADR value is calculated (González et al., 2009; O'Brien et al., 2012).

6
TRANSPORT CORRIDOR

According to the traffic industry, on some important transport routes, one or several bridges have not been upgraded to the required BK. This creates bottlenecks for the heavy transport industry (e.g. steel and timber). The transport sector is forced to either use a higher number of lighter vehicles or detours with heavy vehicles, both resulting in negative environmental and economic effects. Old bridges, not classified with a higher BK, could be strengthened or replaced by new bridges, but this would also result in negative environmental and economic loads on the society. This chapter presents the workflow for a load-carrying capacity assessment in which a transport route called a 'transport corridor' is used. The bridges along the transport corridor are investigated to upgrade the bridges to the required BK, where the last outcome is to strengthen or replace the bridges.

6.1 Process and System Integration

The Swedish Transport Administration released a flowchart model called the 'Four stage principle'. It is used to ensure efficient and sustainable solutions in the agency's daily work (Trafikverket, 2018b). The four stages are as follows:

1. Rethink
2. Optimise
3. Rebuild
4. Build new

The process for the transport corridor was developed to be consistent with the Four stage principle. This process is presented with a flowchart in Figure 6.1, and it consists of five stages. A transport corridor is chosen. Each level is evaluated to determine whether the bridge or bridges of interest along the route can be upgraded to the required BK. The last level results in strengthening or replacing the bridge or bridges. Each stage is explained in detail below.

Inventory. A transport corridor that includes bridges in need of upgrading to a higher BK is selected. It is suggested that this route is selected by the Swedish Transport Administration and the transport and traffic industry. The benefit of this collaboration is that the industry can identify the most important transportation routes. An inventory of bridges along the route is made, and relevant data (e.g. construction drawings) of the road and bridges are collected.

Level 1. The A and B values on the drawings or in the Swedish Transport Administration's database, which is called Bridge and Tunnel Management (BaTMan), for the evaluated bridges are collected. The A and B values are compared with the allowed values specified by the Swedish Transport Administration, which are presented in Chapter 2. Some of the bridges may be upgraded to the BK of interest, and some may not and need to be evaluated more in Level 2.

Level 2. A load-carrying capacity assessment is performed as in Chapter 2.1. The A and B values of the bridges could be increased, as they were evaluated a long time ago and by using a refined structural model, capacity analysis and the safety index method. If the required BK for a bridge is not obtained, more evaluation will be conducted in Level 3.

Level 3. A more rigorous investigation is performed involving one or all of the following methods: condition assessment (not treated in this pre-study), long-term monitoring and numerical model. The last two methods are discussed in detail in Chapter 6.2.

Level 4. If none of the previous levels lead to an upgrade to the required BK for all bridges along the transport corridor, the bridge or bridges will need to be strengthened or replaced. Even if the result is to strengthen a bridge, going through the previous levels can still be an advantage. The investigations may lead to only a few components of the bridge needing to be strengthened, or not as much.

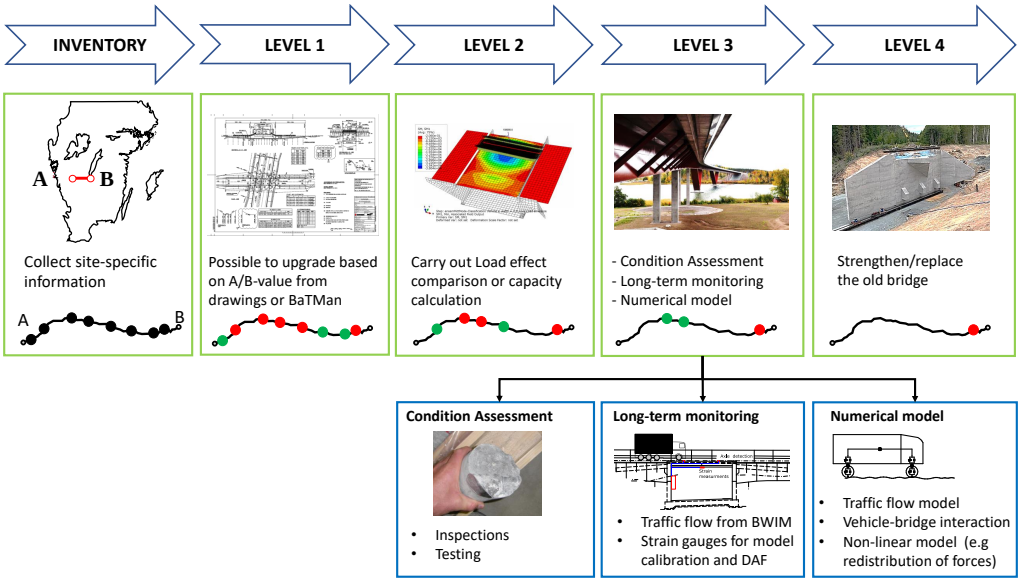

Figure 6.1: Process of load-carrying capacity assessment of existing bridges in a transport corridor.

6.2 Structural Assessment of Bridges

SAMARIS (2006) and González et al. (2009) presented different procedures for the structural assessment of bridges. They proposed the use of long-term monitoring and numerical models. Bridge standards are necessarily conservative, resulting in the replacement or strengthening of a bridge using a traditional assessment. Specific site information leads to a more accurate assessment, resulting in savings of economic and natural resources.

The long-term monitoring strategy is presented in Chapter 5.2. Using long-term monitoring, information such as total strain, axle load, gross weight and vehicle speed can be collected from the actual traffic passing the bridge. This strategy was used by Carlsson and Karoumi (2008) on Ölandsbron (Chapter 2.1), and it resulted in a 27 % increase in B value. González et al. (2009) also monitored the strain (Chapter 4.2). The static strain can be recorded and compared with the total strain by measuring the strain to show the DAF for specific events. González et al. (2009) reported that the DAF decreased with an increase in static strain. Even if the data can only be recorded for a short period, the ADR can be calculated by isolating the vehicle classes and extrapolating the data to extreme values. As presented in Chapter 3.1, several authors have proposed a return period of 1000 years (probability of exceedance of 5 % in 50 years).

Numerical models are another strategy (Chapter 5.3). The distribution of traffic can be monitored using different WIM systems. This information and the bridge properties can be used to perform traffic flow models (e.g. Monte Carlo simulation and static model with influence lines) to identify the worst traffic events. Using vehicle models and their dynamic properties (Chapter 4.3) with road profiles (Chapter 4.1), numerical models can be performed for the worst load scenarios. The results can then be used to calculate the ADR.

The two strategies discussed above can also be used together. Long-term monitoring can be used to record the traffic that enters the transport corridor (e.g. axle spans, gross vehicle weights and location of vehicles in the traffic lanes). This information can be used for all bridges along the corridor when numerical models are performed. In this way, not all bridges will need to be monitored, thus saving money and time.

Conducting a project with a transport corridor and Level 3 also produces important information about the DAF for all bridges in Sweden. This information can be used to investigate the equation that is implemented in the current design code in Sweden (Eq. 2.1 in Chapter 2.1). The literature in Chapter 4.2 shows that the DAF decreases with an increase in gross vehicle weight, consistent with the equation used in Denmark (Scholten et al., 2004).

7

CONCLUSIONS

The following conclusions are drawn based on the literature review and numerical simulations performed within the scope of this pre-study and Bergenudd (2020):

- There is a strong correlation between the load-carrying capacity assessment standard (Trafikverket, 2020) and industry regulations (Transportstyrelsen, 2018b) regarding the configuration of axle systems for vehicles. However, classification vehicles (special vehicles) have heavier gross vehicle weights than the allowed gross vehicle weights for the industry. This indicates the potential to increase the limits for BK1–BK4 to allow heavier gross vehicle weights and/or to upgrade BK1 bridges to BK4, enabling heavier trucks to be used in Sweden.

- Multiple parameters affect DAFs, two of which are road irregularities and trailer suspensions. It has been shown that the DAF increases with increasing road irregularities and stiffer suspension. There is a higher probability of obtaining a higher DAF with steel leaf suspension than with air suspension. Another parameter that has received great attention in the literature is the impact on the DAF from the gross vehicle weight. It has been shown that light vehicles tend to have high DAFs, but it is not light vehicles that create critical load effects, and they are therefore not relevant from a design perspective. However, heavy vehicles have DAFs that are critical for design. Both experimental and analytical investigations have shown that heavy gross vehicle weights result in low DAF values.

- Equations have been presented, used in different countries to calculate DAFs. Most of them (including the Swedish one) have been empirical, with the span length being the only unknown variable. However, the literature has presented a consistent trend: An increase in gross vehicle weight results in a decreased DAF. The only known design code including this trend is the Danish RBBA code (Scholten et al., 2004). Introducing gross vehicle weight as a variable in the Swedish design code could result in heavier trucks being allowed on Swedish bridges.

- At the start of this project, one objective was to investigate if different DAFs could be used for different limit states. In the reviewed literature, this is not an objective that is mentioned or investigated. The equation used to calculate the IF in each country is mostly the same. It can vary depending on the span

length, bridge type and or fundamental frequency. However, no information in the design codes has been found on how the equations consider different limit states.

- Multiple authors have stated that existing design codes for load-carrying capacity assessments are conservative regarding traffic loads and their dynamic amplification. The consequences of this are that the full capacities of bridges are not utilised or that bridges need to be strengthened or replaced. This pre-study has presented effective ways to collect site-specific dynamic traffic load information and a methodology to produce site-specific dynamic allowances using both experimental measurements and numeric models. The results of the studies have shown that a significantly lower design DAF, compared with the predefined values of design codes (including the Swedish one), can be obtained. In one case, the Swedish proposed DAF overestimated the real one by almost 24 %.

- Even if a site-specific assessment should be performed in Sweden, is it difficult to know how traffic loading events should be evaluated. The Swedish design code (Trafikverket, 2020) states that clients can allow the use of the safety index method, which is a probabilistic analysis with a return period of one year. However, the code gives no guidelines regarding traffic load data. Can both experimental measurements and numerical models be used? If a BK1 bridge is upgraded to a BK4 bridge, is it permissible to use a monitored traffic flow model from another location where BK4 vehicles are passing? It has been shown that site-specific assessment is an effective evaluation method, but to encourage its use and to ensure that all assessments are performed in the same way, guidelines must be provided by Swedish government agencies.

- The traffic industry has reported that, on some important transport routes, one or several bridges have not been upgraded to the required BK. This creates bottlenecks for the heavy transport (e.g. steel and timber) industries. The transport sector is forced to either use greater numbers of light vehicles or detours with heavy vehicles, which both result in negative environmental and economic effects. Conducting a pilot test along a transport corridor with bridges of interest could lead to an increase in the load-carrying capacity of the bridges, which would otherwise have to be strengthened or replaced. The intention is to perform a detailed site-specific evaluation based on a five-stage flowchart.

The introduction to this pre-study (Chapter 1.1) stated that the goal of the Swedish Transport Administration is to classify 70–80 % of the strategic road network for the heavy transport industry as BK4 by 2029. To reach this goal, it is estimated that over 700 bridges will need to be strengthened or replaced. Based on the conclusions presented previously, the authors of this pre-study believe that some of the bridges can be upgraded to BK4 without the need for strengthening or replacement, which would result in economic and environmental benefits for the industry and society.

8

RESEARCH PROPOSALS

The pre-study findings have resulted in the research proposals presented in this section. The authors believe that several topics can be covered within the framework of a PhD project.

Site-Specific Field Measurements to Quantify DAFs

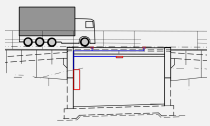

The field measurements used by the ARCHES and SAMARIS projects have shown promising results, particularly for determining site-specific DAFs (see Chapter 5). Therefore, is it proposed that similar techniques should be further developed and adopted for the Swedish vehicle fleet.

Guidelines for Numerical Modelling of VBIs

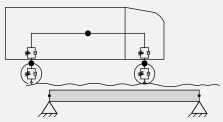

Extensive research has been carried out over the past century to understand and develop models for VBIs. It is proposed that these findings could be summarised in a set of design guidelines that can be used by designers to determine DAFs.

DAF for Each Limit State

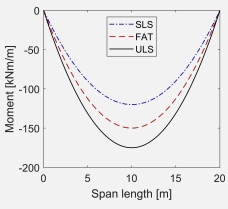

In the reviewed literature and design codes, no information has been found if different DAFs could be used for the different limit states and what impact that would have on the load-capacity. It is of interest to investigate if a lower DAF could be used for some of the limit states, which could result in a higher load-capacity for bridges.

Three-Dimensional Analysis of VBIs

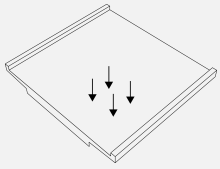

The numerical results presented in this work are mainly based on 2D Euler–Bernoulli beam theory. This is normally a good approximation for long-span bridges or in resonance situations. In reality, however, most bridges are short-span bridges that require a 3D shell model. This could, for example, be implemented in Abaqus by writing a user subroutine.

Introduce Gross Vehicle Weight in DAF Equations

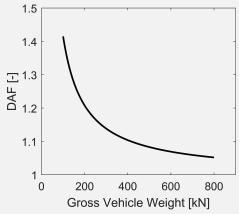

Chapter 3 presented the equations used in different countries to calculate DAFs. Most of the equations, including the Swedish one, are empirical, with the span length as the only unknown variable. However, the literature has presented a consistent trend: An increase in gross vehicle weight results in a decreased DAF. The only known design code to include this trend is the Danish RBBA code. Introducing gross vehicle weight as a variable in the Swedish design code could result in heavier trucks being allowed on Swedish bridges, providing economic and environmental benefits.

Pilot Test of Proposed Framework for Transport Corridors

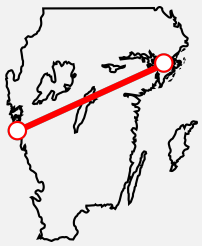

Chapter 6 proposed a pilot test to verify whether the framework for transport corridors could be used to increase the load-carrying capacities of structures that would otherwise have to be strengthened or replaced. Several reports have shown that there are both economic and environmental benefits of performing load-carrying capacity assessments with site-specific data, such as traffic flow data and DAF values, which could result in an increased maximum allowable gross weight for trucks.

Bibliography

AASHTO, 1989. Standard specifications for highway bridges. No. 14. American Association of State Highway and Transportation Officials, Washington, D.C.

AASHTO, 2012. LRFD bridge design specifications. No. 6. American Association of State Highway and Transportation Officials, Washington, D.C.

Bakht, B., Pinjarkar, S., 1989. Dynamic testing of highway bridges–a review. Transportation Research Record (1223), 93–100.

Bergenudd, J., 2020. Refined model for calculating the dynamic amplification factor for road bridges. TVSM-5000.

Bien, J., Elfgren, L., Olofsson, J., 2007. Sustainable bridges: Assessment for Future Traffic Demands and Longer Lives. Dolnoslaskie Wydawnictwo Edukacyjne.

Billing, J., Green, R., 1984. Design provisions for dynamic loading of highway bridges. Transportation research record (950), 94–103.

Cantero, D., Arvidsson, T., OBrien, E., Karoumi, R., 2016. Train–track–bridge modelling and review of parameters. Structure and Infrastructure Engineering 12 (9), 1051–1064.

Cantero, D., González, A., O'Brien, E. J., 2011. Comparison of bridge dynamic amplification due to articulated 5-axle trucks and large cranes. Baltic Journal of Road and Bridge Engineering 6 (1), 39–47.

Cantero, D., O'Brien, E. J., González, A., 2010. Modelling the vehicle in vehicle—infrastructure dynamic interaction studies. Proceedings of the Institution of Mechanical Engineers, Part K: Journal of Multi-body Dynamics 224 (2), 243–248.

Cantieni, R., 1983. Dynamic load tests on highway bridges in switzerland. Rep 211.

Caprani, C. C., 2012. Calibration of a congestion load model for highway bridges using traffic microsimulation. Structural Engineering International 22 (3), 342–348.

Caprani, C. C., 2013. Lifetime highway bridge traffic load effect from a combination of traffic states allowing for dynamic amplification. Journal of Bridge Engineering 18 (9), 901–909.

Caprani, C. C., González, A., Rattigan, P. H., OBrien, E. J., 2012. Assessment dynamic ratio for traffic loading on highway bridges. Structure and Infrastructure Engineering 8 (3), 295–304.

Carey, C., OBrien, E. J., Malekjafarian, A., Lydon, M., Taylor, S., 2017. Direct field measurement of the dynamic amplification in a bridge. Mechanical Systems and Signal Processing 85, 601–609.

Carlsson, F., Karoumi, R., 2008. Probabilistisk analys av Ölandsbron baserad på fordonens verkliga laster och sidopositioner. TRITA-BKN 127.

Chan, T. H. T., O'Connor, C., 1990. Wheel loads from highway bridge strains: field studies. Journal of structural engineering 116 (7), 1751–1771.

Deng, L., Yu, Y., Zou, Q., Cai, C., 2015. State-of-the-art review of dynamic impact factors of highway bridges. Journal of Bridge Engineering 20 (5), 04014080.

DIVINE, 1998. Dynamic interaction between vehicles and infrastructure experiment: technical report. Organization for Economic Co-operation and Development (OECD). Road Transport Research. Scientific Expert Group. Paris.

Dodds, C. J., 1972. BSI proposals for generalized terrain dynamic inputs to vehicles. No. 5. International Organization for Standardization ISO/TC/108/WG9.

Emanuelsson, P., Persson, A., 2011. Probabilistisk säkerhetsverifiering av befintlig vägbro. TVBK - 5192.

EN 1991-2, 2002. Eurocode 1: Actions on structures-Part 2: Traffic loads on bridges. European Committee for Standardisation.

ENV 1991-3, 1994. Traffic Loads on Bridges. European Committee for Standardisation.

Goenaga, B., Fuentes, L., Mora, O., 2017. Evaluation of the methodologies used to generate random pavement profiles based on the power spectral density: an approach based on the international roughness index. Ingeniería e Investigación 37 (1), 49–57.

González, A., 2001. Development of Accurate Methods of Weighing Trucks in Motion. Thesis (PhD). Ireland: Department of Civil Engineering, Trinity College Dublin.

González, A., O'Brien, E. J., McGetrick, P., 2010. Detection of bridge dynamic parameters using an instrumented vehicle. In: 5th World Conference on Structural Control and Monitoring, 12th-14th July, Tokyo, Japan. World Conference on Structural Control and Monitoring.

González, A., Znidaric, A., Casas, J. R., O'Brien, E. J., et al., 2009. Eu fp6-arches deliverable d10: Recommendations on dynamic amplification allowance. Tech. rep., FEHRL.

Hillerborg, A., 1951. Dynamic influences of smoothly running loads on simply supported girders. No. 68. Esselte.

Huang, D., Wang, T.-L., Shahawy, M., 1993. Impact studies of multigirder concrete bridges. Journal of Structural Engineering 119 (8), 2387–2402.

Hwang, E.-S., Nowak, A. S., 1991. Simulation of dynamic load for bridges. Journal of structural engineering 117 (5), 1413–1434.

ISO, 2016. Mechanical vibration - Road surface profiles - Reporting of measured data, ISO 8608:2016. International Organization for Standardisation.

Kalman, B., Ullberg, J., 2020. Bärighetsklass BK4 – hur påverkas det äldre vägnätet? Bygg&Teknik. https://byggteknikforlaget.se/barighetsklass-bk4-hur-paverkas-det-aldre-vagnatet/, accessed: 2021-09-16.

Kriloff, A., 1905. Über die erzwungenen schwingungen von gleichförmigen elastischen stäben. Mathematische Annalen 61 (2), 211–234.

Ludescher, H., Brühwiler, E., 2009. Dynamic amplification of traffic loads on road bridges. Structural engineering international 19 (2), 190–197.

Lydon, M., Taylor, S. E., Robinson, D., Callender, P., Doherty, C., Grattan, S. K., O'Brien, E. J., 2014. Development of a bridge weigh-in-motion sensor: performance comparison using fiber optic and electric resistance strain sensor systems. IEEE Sensors Journal 14 (12), 4284–4296.

Malekjafarian, A., 2016. On the use of drive-by measurement for indirect bridge monitoring.

McGetrick, P., Kim, C.-W., González, A., et al., 2013. Dynamic axle force and road profile identification using a moving vehicle. International Journal of Architecture, Engineering and Construction 2 (1), 1–16.

McLean, D. I., Marsh, M. L., 1998. Dynamic impact factors for bridges. Vol. 266. Transportation Research Board.

MTPRC, 1989. General code for design of highway bridges and culverts. Ministry of Transportof the People's Republic of China, Beijing.

MTPRC, 2004. General code for design of highway bridges and culverts. Ministry of Transportof the People's Republic of China, Beijing.

Natanaelsson, K., Eriksson, T., 2020. Regeringsuppdrag: Implementering av bärighetsklass 4. Swedish Transport Administration (Trafikverket).

Natanaelsson, K., Ngo, P., 2015. Regeringsuppdrag: Fördjupade analyser av att tillåta tyngre fordon på det allmänna vägnätet. Swedish Transport Administration (Trafikverket).

Nowak, A. S., 1993. Live load model for highway bridges. Structural safety 13 (1-2), 53–66.

Nowak, A. S., Hong, Y.-K., 1991. Bridge live-load models. Journal of Structural Engineering 117 (9), 2757–2767.

O'Brien, E. J., Cantero, D., Enright, B., González, A., 2010. Characteristic dynamic increment for extreme traffic loading events on short and medium span highway bridges. Engineering Structures 32 (12), 3827–3835.

O'Brien, E. J., Caprani, C. C., 2005. Headway modelling for traffic load assessment of short to medium span bridges. The Structural Engineer 83 (16), 33–36.

O'Brien, E. J., González, A., Znidaric, A., 2012. Recommendations for dynamic allowance in bridge assessment. In: Bridge Maintenance, Safety Management and Life-Cycle Optimization, Sixth International IABMAS Conference, Stresa, Lake Maggiore, Italy, 8-12 July 2012. CRC Press.

Patel, V., Vinay, K., 2020. Implementation of on-board weighing system for trailer application. International Journal of Engineering Science and Technology 7 (1), 32–37.

Paultre, P., Chaallal, O., Proulx, J., 1992. Bridge dynamics and dynamic amplification factors — a review of analytical and experimental findings. Canadian Journal of Civil Engineering 19 (2), 260–278.

Plos, M., 2002. Improved bridge assessment using non-linear finite element analyses. In: Bridge Maintenance, Safety and Management. pp. 133–134.

Plos, M., Johansson, M., Zandi, K., Shu, J., 2021. Recommendations for Assessment of Reinforced Concrete Slabs: Enhanced structural analysis with the finite element method. Chalmers University of Technology.

Radoičić, G., Jovanović, M., Arsić, M., 2016. Experience with an on-board weighing system solution for heavy vehicles. Etri Journal 38 (4), 787–797.

SAMARIS, 2006. Guidance for the optimal assessment of highway structures. Final Report to the European Commission.

Scholten, C., Enevoldsen, I., Arnbjerg-Nielsen, T., Randrup-Thompsen, S., Sloth, M., Engelund, S., Faber, M., 2004. Reliability-Based Classification of the Load Carrying Capacity of Existing Bridges-Guideline Document (Report 291). Road Directorate, Copenhagen.

Stokes, S. G. G., 1849. Discussion of a differential equation relating to the breaking of railway bridges. Printed at the Pitt Press by John W. Parker.

Svedholm, C., 2017. Efficient modelling techniques for vibration analyses of railway bridges. Ph.D. thesis, KTH Royal Institute of Technology.

Tilly, G., 1986. Dynamic behaviour of concrete structures report of the rilem 65-mdb committee. Materials and Structures 19 (6), 460–460.

Timoshenko, S., 1922. On the forced vibrations of bridges. The London, Edinburgh, and Dublin Philosophical Magazine and Journal of Science 43 (257), 1018–1019.

Trafikverket, 2018a. Brobärighet för att kunna upplåtas för bärighetsklass BK4. Vol. TRV 2018/113. Swedish Transport Administration (Trafikverket).

Trafikverket, 2018b. Fyrstegsprincipen. Swedish Transport Administration (Trafikverket). https://www.trafikverket.se/for-dig-i-branschen/Planera-och-utreda/Planerings--och-analysmetoder/fyrstegsprincipen/, accessed: 2021-07-19.

Trafikverket, 2019. Fler vägar för 74-tons-lastbilar i mellersta Sverige. Swedish Transport Administration (Trafikverket). https://www.trafikverket.se/om-oss/pressrum/pressmeddelanden/lansvisa-pressmeddelande/Dalarna/2019/fler-vagarfor-74-tonslastbilar-i-mellersta-sverige/, accessed: 2021-09-16.

Trafikverket, 2020. Bärighetsberäkning av broar - KRAV. Publikation TDOK 2013:0267. Vol. 7.0. Swedish Transport Administration (Trafikverket).

Transportstyrelsen, 2018a. Transportstyrelsen författningssamling: Transportstyrelsens föreskrifter och allmänna råd om tillämpning av eurokoder. Publikation TSFS 2018:57. Swedish Transport Agency (Transportstyrelsen).

Transportstyrelsen, 2018b. Legal loading: Weight and dimension regulations for heavy vehicles. Publication TS201616. Swedish Transport Agency (Transportstyrelsen).

Tyan, F., Hong, Y.-F., Tu, S.-H., Jeng, W. S., et al., 2009. Generation of random road profiles. Journal of Advanced Engineering 4 (2), 1373–1378.

Vägverket, 1998. Allmän teknisk beskrivning för Klassningsberäkning av vägbroar. Publikation 1998:78. Vägverket, Borlänge, Sweden.

Vägverket, 2004. BWIM-mätningar 2002 och 2003: Slutrapport. VVPubl 2003:165. Vägverket, Borlänge, Sweden.

Vägverket, 2006. BWIM-mätningar 2004 och 2005: Projektrapport. VVPubl 2006:136. ISSN 1401-9612. Vägverket, Borlänge, Sweden.

Volvo Lastvagnar, 2018. Volvo Lastvagnar levererar 90-tons malmlastbilar till svensk gruvsatsning. Volvo Lastvagnar. https://www.volvotrucks.se/sv-se/news/press-releases/2018/mar/pressrelease-180321.html, accessed: 2021-09-16.

Wang, T., Shahawy, M., Huang, D., 1993. Dynamic response of highway trucks due to road surface roughness. Computers & structures 49 (6), 1055–1067.

Willis, R., 1849. Report of the Commissioners Appointed to Inquire Into the Application of Iron to Railway Structures. In: Grey, G. (Ed.), Preliminary essay to the appendix B: experiment for determining the effects produced by causing weights to travel over bars with different velocities. William Clowes and Sons, London.

Yang, Y.-B., Yau, J., Yao, Z., Wu, Y., 2004. Vehicle-bridge interaction dynamics: with applications to high-speed railways. World Scientific.

Zhang, Y., Zhao, Q., Liang, X., Qiao, H., 2021. Design of on-board weighing system based on stm32. International Journal of Scientific Advances 2 (2), 141–142.

Žnidarič, A., Lavrič, I., 2010. Applications of b-wim technology to bridge assessment. In: Fifth International Conference on Bridge Maintenance, Safety and Management, IABMAS.

Žnidarič, A., Lavrič, I., Kalin, J., 2005. Nothing-on-the-road axle detection with threshold analysis. In: International Conference on Weigh-In-Motion, 4th, 2005, Taipei, Taiwan.

Žnidarič, A., Lavrič, I., Kalin, J., 2008. Measurements of bridge dynamics with a bridge weigh-in-motion system. In: 5th International Conference on Weigh-in-Motion (ICWIM5). pp. 388–397.

A
Appendix 1

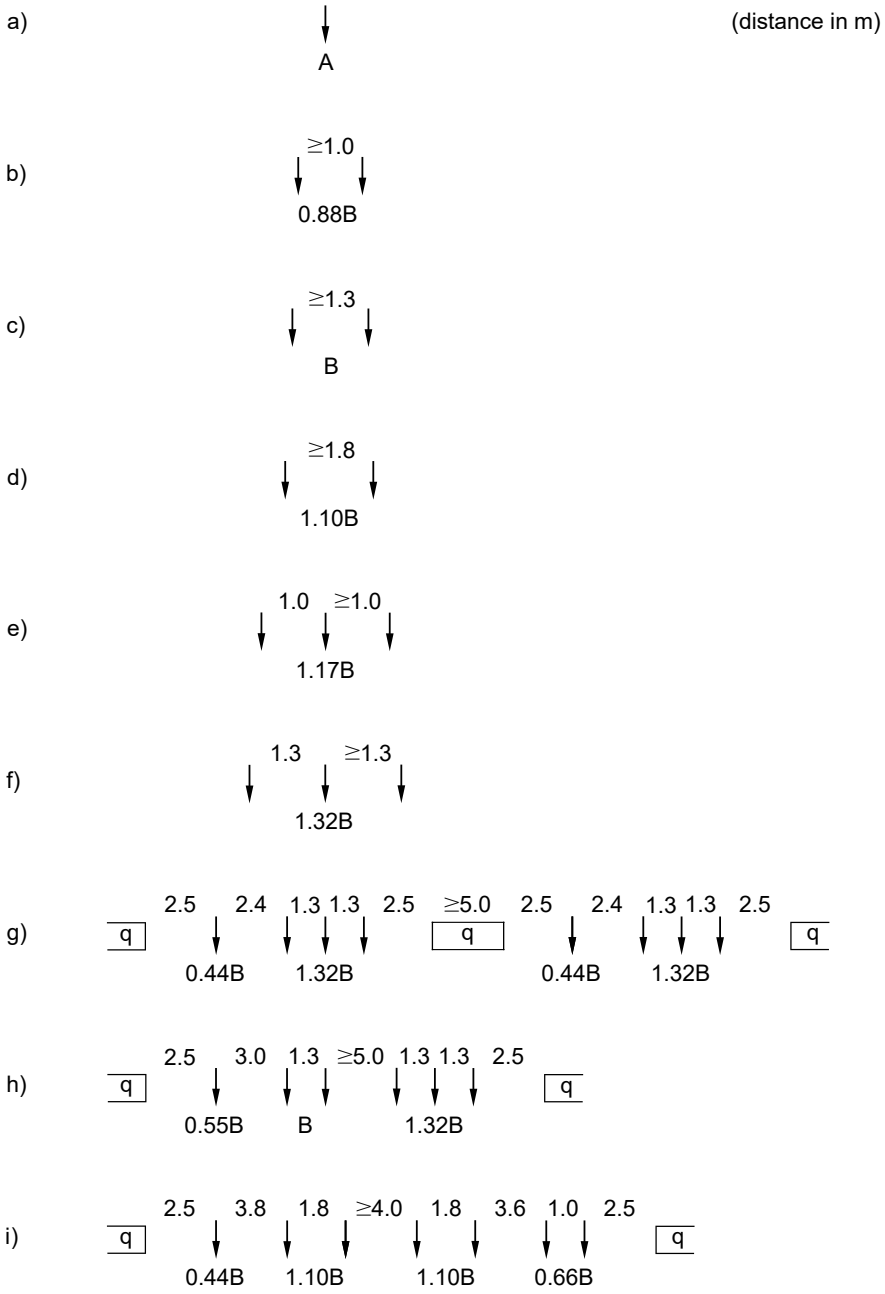

Figure A.1: Special vehicle a)-i), reproduced from Trafikverket (2020).

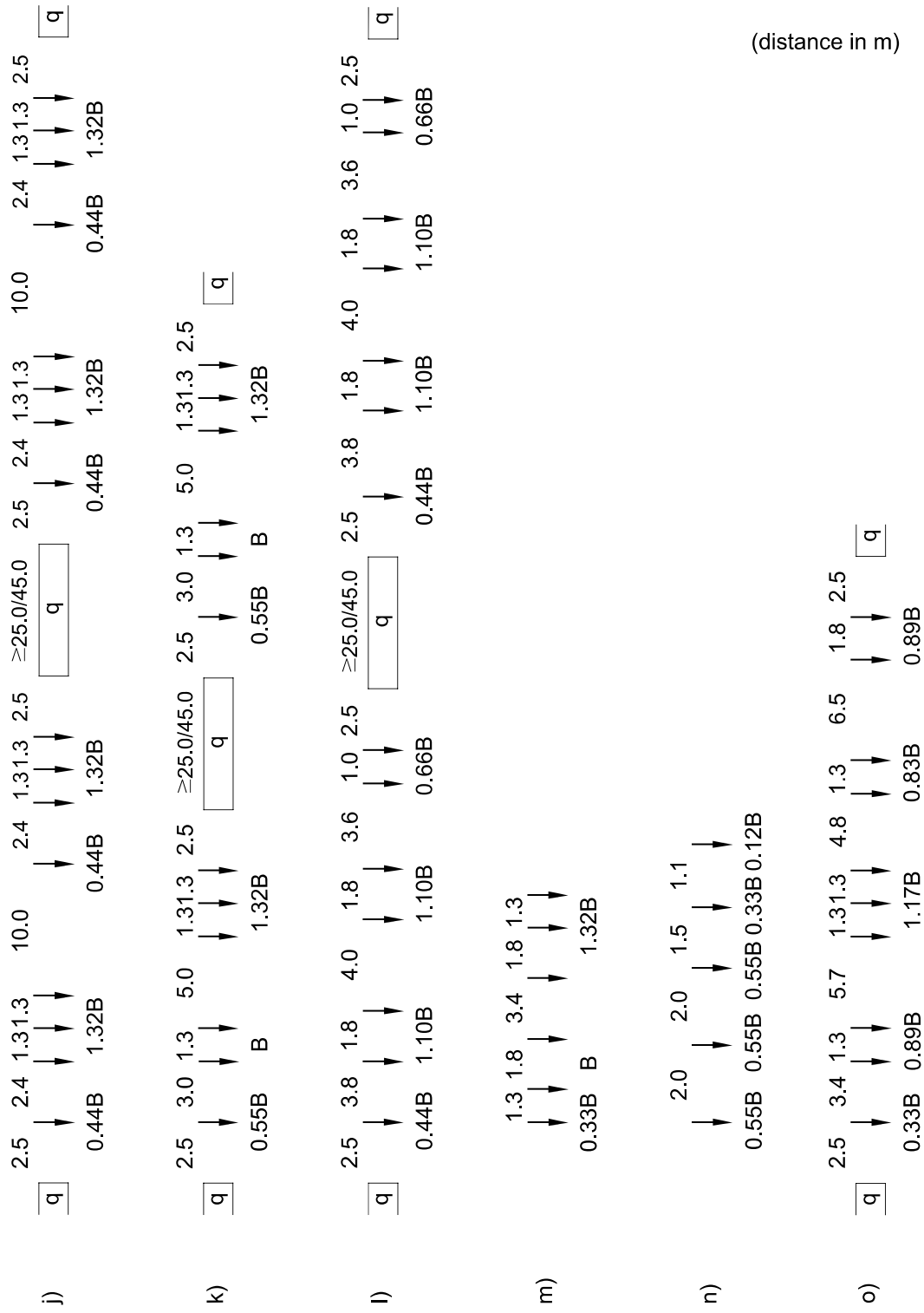

Figure A.2: Special vehicle j)-o), reproduced from Trafikverket (2020).

DEPARTMENT OF ARCHITECTURE AND CIVIL ENGINEERING
CHALMERS UNIVERSITY OF TECHNOLOGY
Gothenburg, Sweden
www.chalmers.se

CHALMERS
UNIVERSITY OF TECHNOLOGY